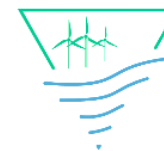




**COPPE**

Instituto Alberto Luiz Coimbra de  
Pós-Graduação e Pesquisa de Engenharia

**UFRJ**



**GERO**

GRUPO DE ENERGIA RENOVÁVEL  
NO OCEANO

# URANS simulations of a horizontal axis wind turbine under stall condition using Reynolds stress turbulence models

**Candidate:** Mojtaba Maali Amiri

**Supervisor:** Prof. Segen F. Estefen

**July 2020**

# Outline:

## 1. Introduction

1.1. Problem Definition and Scope of the Present Work

1.2. Literature Review

1.3. Research Objectives

## 2. Methodology

2.1. Numerical Model

2.2. Wind Turbine Model and Computational Conditions

2.4. Computational Domain and Boundary Conditions and Grid

## 3. Verification

## 4. Results and Discussion

## 5. Conclusions and Future Works

## 6. Contributions

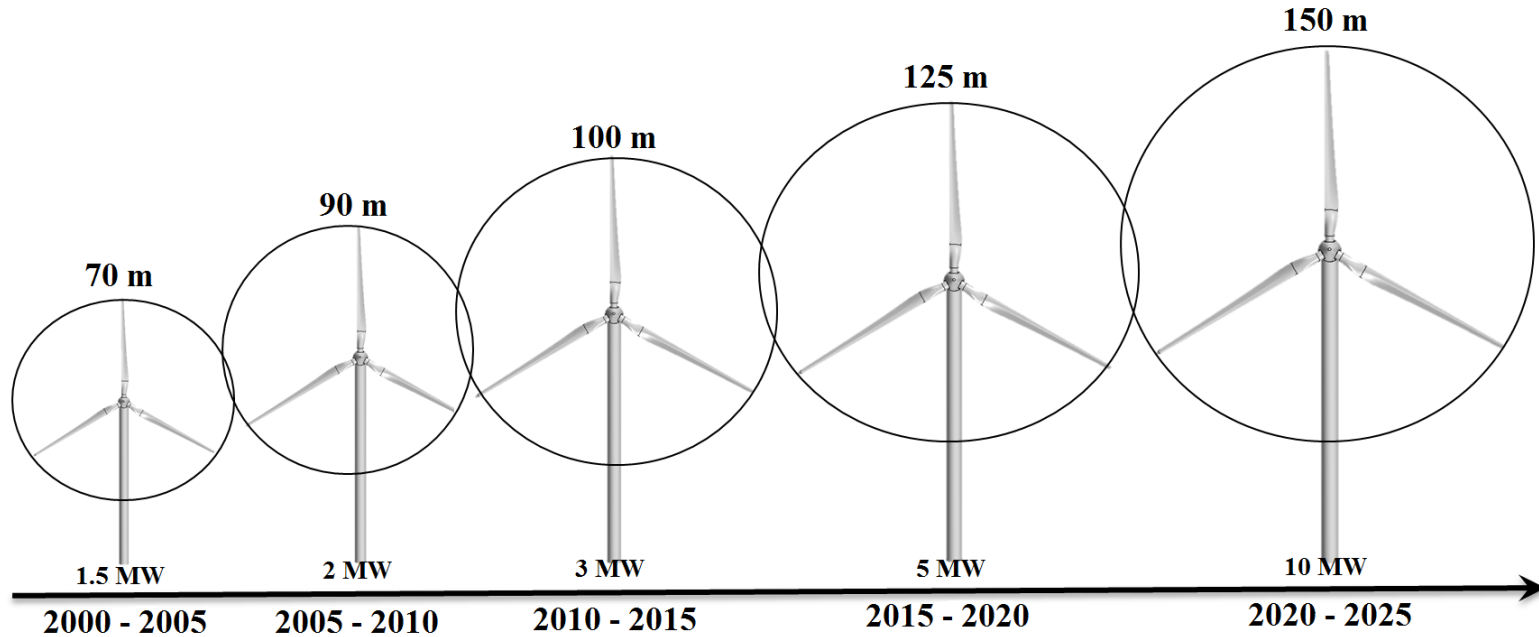
# Problem Definition:

Evolution of the wind turbine size:

P. Veers (2019), J. O'Brien et al. (2017), W. Zhang et al. (2012), Hansen and Madsen (2011), E. Echavarria (2009)

# Problem Definition:

## Evolution of the wind turbine size:

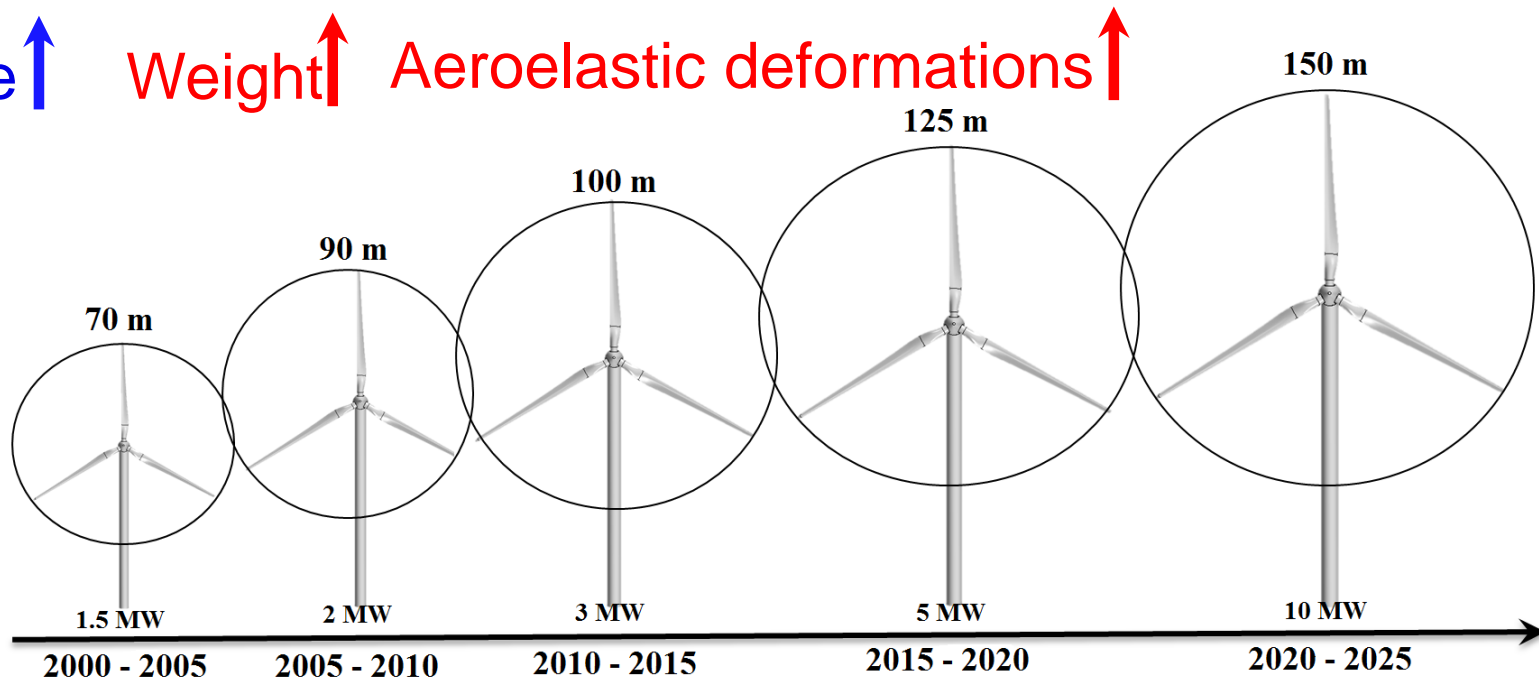


P. Veers (2019), J. O'Brien et al. (2017), W. Zhang et al. (2012), Hansen and Madsen (2011), E. Echavarria (2009)

# Problem Definition:

## Evolution of the wind turbine size:

Size ↑    Weight ↑    Aeroelastic deformations ↑

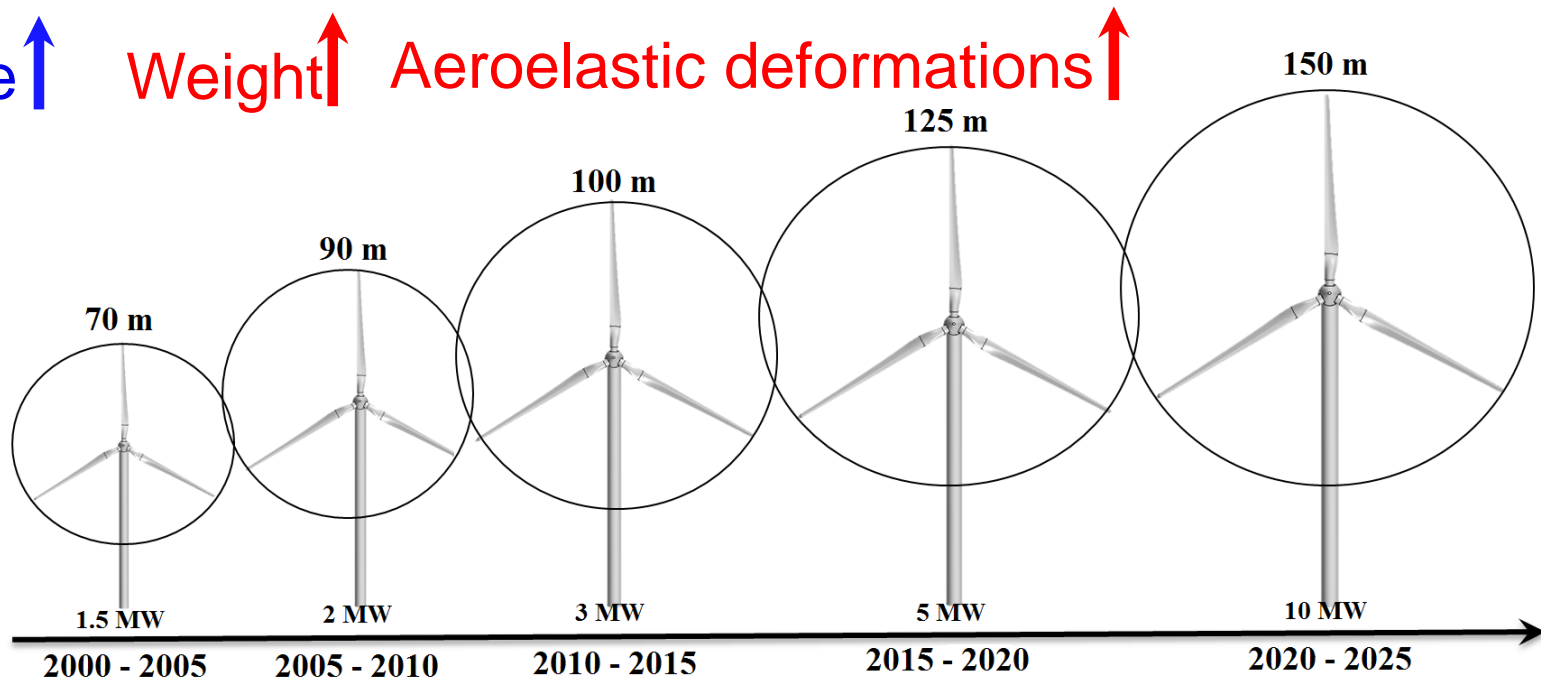


P. Veers (2019), J. O'Brien et al. (2017), W. Zhang et al. (2012), Hansen and Madsen (2011), E. Echavarria (2009)

# Problem Definition:

## Evolution of the wind turbine size:

Size ↑    Weight ↑    Aeroelastic deformations ↑



Modeling accuracy of the turbulent flow around the wind turbine rotors

P. Veers (2019), J. O'Brien et al. (2017), W. Zhang et al. (2012), Hansen and Madsen (2011), E. Echavarria (2009)

## Problem Definition:

Modeling the turbulent flow around a wind turbine:

$$\frac{\partial(\rho U_i)}{\partial t} + \frac{\partial(\rho U_j U_i)}{\partial x_j} = -\frac{\partial P}{\partial x_i} + \frac{\partial(2\mu S_{ij})}{\partial x_j}$$

C. Argyropoulos and N. Markatos (2015)

## Problem Definition:

Modeling the turbulent flow around a wind turbine:

$$\frac{\partial(\rho U_i)}{\partial t} + \frac{\partial(\rho U_j U_i)}{\partial x_j} = -\frac{\partial P}{\partial x_i} + \frac{\partial(2\mu S_{ij})}{\partial x_j}$$

CFD

C. Argyropoulos and N. Markatos (2015)



## Problem Definition:

Modeling the turbulent flow around a wind turbine:

$$\frac{\partial(\rho U_i)}{\partial t} + \frac{\partial(\rho U_j U_i)}{\partial x_j} = -\frac{\partial P}{\partial x_i} + \frac{\partial(2\mu S_{ij})}{\partial x_j}$$

CFD

URANS

C. Argyropoulos and N. Markatos (2015)

## Problem Definition:

Modeling the turbulent flow around a wind turbine:

$$\frac{\partial(\rho U_i)}{\partial t} + \frac{\partial(\rho U_j U_i)}{\partial x_j} = -\frac{\partial P}{\partial x_i} + \frac{\partial(2\mu S_{ij})}{\partial x_j}$$

CFD

### URANS

1. Reynolds stress turbulence models
2. Nonlinear quadratic and cubic turbulent eddy viscosity models
3. Linear turbulent eddy viscosity models

C. Argyropoulos and N. Markatos (2015)

## Problem Definition:

Modeling the turbulent flow around a wind turbine:

$$\frac{\partial(\rho U_i)}{\partial t} + \frac{\partial(\rho U_j U_i)}{\partial x_j} = -\frac{\partial P}{\partial x_i} + \frac{\partial(2\mu S_{ij})}{\partial x_j}$$

CFD

### URANS

1. Reynolds stress turbulence models
2. Nonlinear quadratic and cubic turbulent eddy viscosity models
3. Linear turbulent eddy viscosity models

↑ Computational cost  
And  
Accuracy

C. Argyropoulos and N. Markatos (2015)

## Problem Definition:

Modeling the turbulent flow around a wind turbine:

$$\frac{\partial(\rho U_i)}{\partial t} + \frac{\partial(\rho U_j U_i)}{\partial x_j} = -\frac{\partial P}{\partial x_i} + \frac{\partial(2\mu S_{ij})}{\partial x_j}$$

## CFD

URANS

1. Reynolds stress turbulence models
2. Nonlinear quadratic and cubic turbulent eddy viscosity models
3. Linear turbulent eddy viscosity models



Computational cost

And

Accuracy

The choice of a proper turbulence model is a compromise between the accuracy and the computational effort.

C. Argyropoulos and N. Markatos (2015)

## Problem Definition:

Modeling the turbulent flow around a wind turbine:

$$\frac{\partial(\rho U_i)}{\partial t} + \frac{\partial(\rho U_j U_i)}{\partial x_j} = -\frac{\partial P}{\partial x_i} + \frac{\partial(2\mu S_{ij})}{\partial x_j}$$

CFD

URANS

1. Reynolds stress turbulence models
2. Nonlinear quadratic and cubic turbulent eddy viscosity models
3. Linear turbulent eddy viscosity models



Computational cost

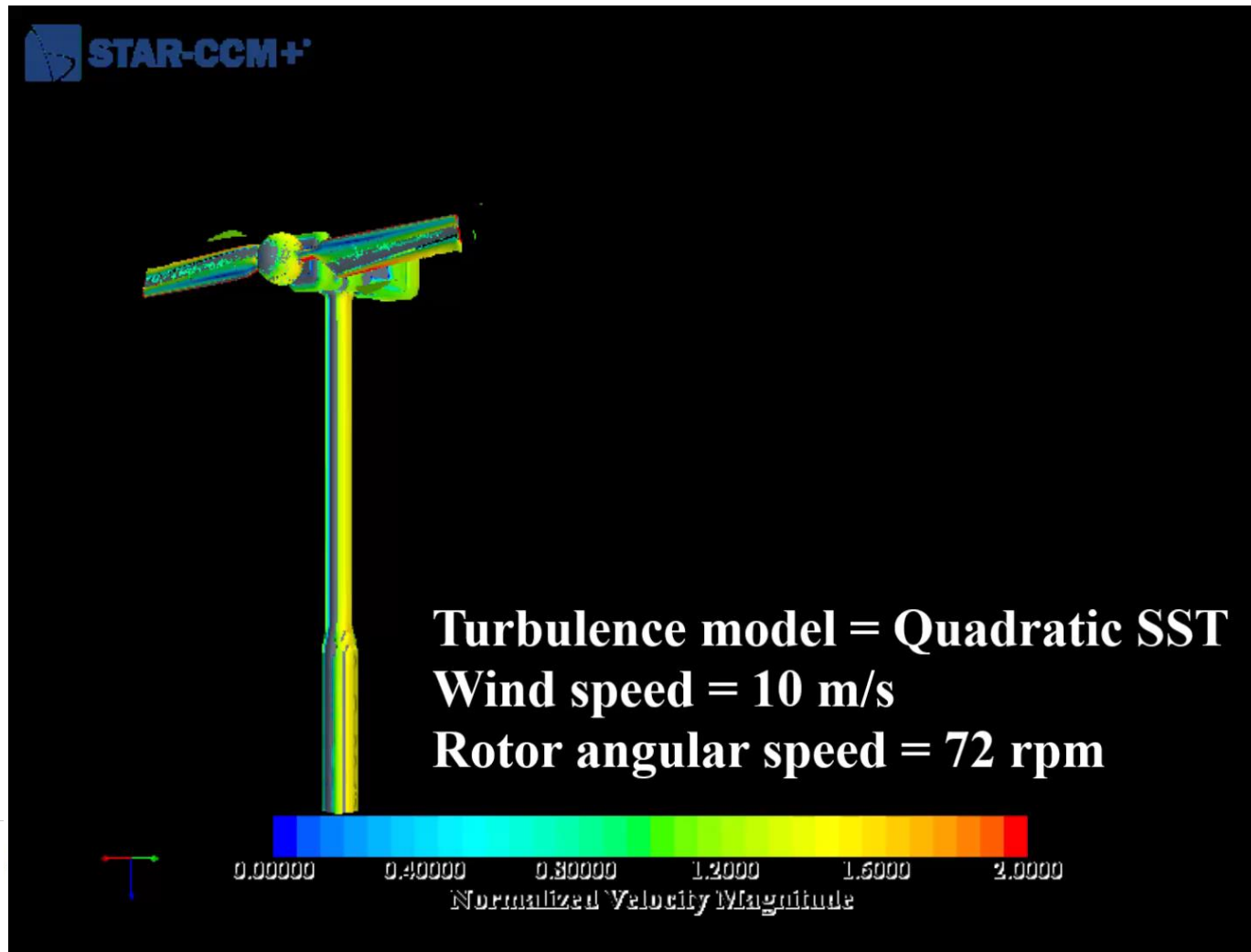
And

Accuracy

The choice of a proper turbulence model is a compromise between the accuracy and the computational effort.

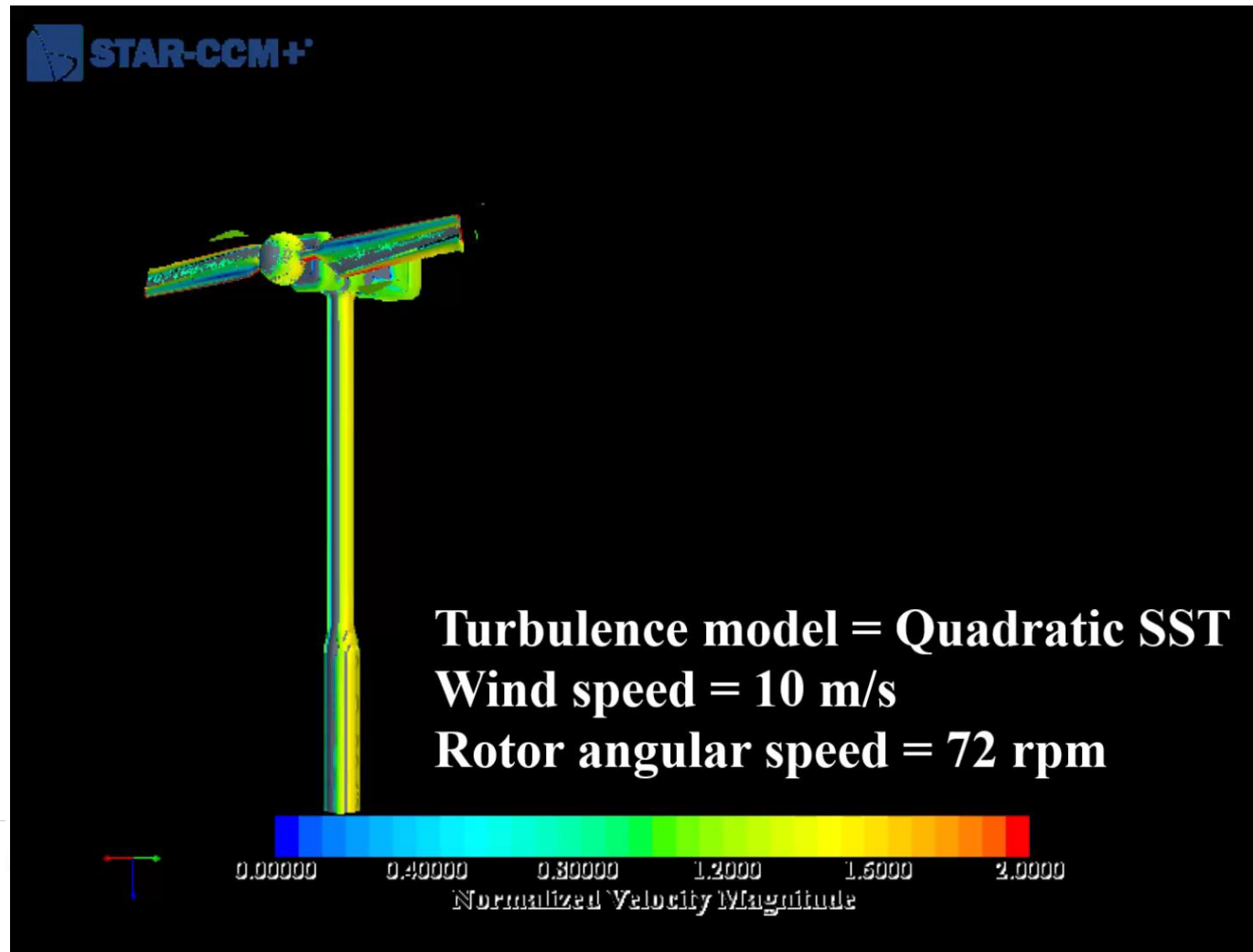
C. Argyropoulos and N. Markatos (2015)

# Problem Definition:



# Problem Definition:

Correct prediction of the turbulent flow characteristics around  
wind turbines operating under stall condition



## Scope of the Present Work:

- Evaluation of the capabilities of five URANS-based turbulence models to predict the turbulent flow characteristics around a horizontal axis wind turbine operating under stall condition.



# Literature Review:

The use of nonlinear eddy viscosity and Reynolds stress turbulence models

S. A. Abdulqadir et al. (2017)

# Literature Review:

## The use of nonlinear eddy viscosity and Reynolds stress turbulence models

S. A. Abdulqadir et al. (2017)

F. Carneiro (2019), H. Wang et al. (2019), H. Rahimi et al. (2018),  
A. Ebrahimi and M. Movahhedi (2018), M. Moshfeghi et al. (2017), H. Rahimi et al. (2016),  
M. Nobari et al. (2016), M. Make and G. Vaz (2015), S. Guntur and N. N. Sørensen (2015),  
L. Daroczy (2015), J. Y. You et al. (2013), Q. Wang et al. (2012), G. Yu et al. (2011),  
N. Tachos (2010), A. Spentzos et al. (2007), N. N. Sørensen et al. (2002), H. Snel (1998, 2003),

linear  $k - \omega$  SST

# Literature Review:

The use of nonlinear eddy viscosity and Reynolds stress turbulence models

S. A. Abdulqadir et al. (2017)

# Literature Review:

## The use of nonlinear eddy viscosity and Reynolds stress turbulence models

S. A. Abdulqadir et al. (2017)

1. The latest formulations of the turbulence models are not considered.
2. Lack of detailed information about the computational cost of each turbulence model.
3. It neglects the influence of the tower.

# Research Objectives:

- ❑ Extending the knowledge of the turbulent flow characteristics around horizontal axis wind turbines.
- ❑ Assessing the performance of five URANS turbulence models, principally Reynolds stress models, in predicting the wind turbines aerodynamics under stall condition.

# Numerical Model:

# Numerical Model:

- ❑ STARCCM+ is used.
- ❑ Modeling the fluid flow:

$$\frac{\partial(\rho U_i)}{\partial t} + \frac{\partial(\rho U_j U_i)}{\partial x_j} = -\frac{\partial P}{\partial x_i} + \frac{\partial(2\mu S_{ij} + \tau_{ij})}{\partial x_j},$$

with continuity:

$$\frac{\partial U_i}{\partial x_i} = 0,$$

# Numerical Model:

□ STARCCM+ is used.

□ Five turbulence models are used:

□ Modeling the fluid flow:

$$\frac{\partial(\rho U_i)}{\partial t} + \frac{\partial(\rho U_j U_i)}{\partial x_j} = -\frac{\partial P}{\partial x_i} + \frac{\partial(2\mu S_{ij} + \tau_{ij})}{\partial x_j},$$

with continuity:

$$\frac{\partial U_i}{\partial x_i} = 0,$$



# Numerical Model:

□ STARCCM+ is used.

□ Modeling the fluid flow:

$$\frac{\partial(\rho U_i)}{\partial t} + \frac{\partial(\rho U_j U_i)}{\partial x_j} = -\frac{\partial P}{\partial x_i} + \frac{\partial(2\mu S_{ij} + \tau_{ij})}{\partial x_j},$$

with continuity:

$$\frac{\partial U_i}{\partial x_i} = 0,$$

□ Five turbulence models are used:

1. Reynolds stress turbulence model
  - 1.1. Linear pressure-strain model (LRST)
  - 1.2. Quadratic pressure-strain model (QRST)
  - 1.3. Elliptic blending pressure-strain model (ERST)
2. SST k-w turbulence model
  - 2.1. Linear eddy viscosity SST k-w
  - 2.2. Quadratic nonlinear SST k-w

# Numerical Model:

□ STARCCM+ is used.

□ Modeling the fluid flow:

$$\frac{\partial(\rho U_i)}{\partial t} + \frac{\partial(\rho U_j U_i)}{\partial x_j} = -\frac{\partial P}{\partial x_i} + \frac{\partial(2\mu S_{ij} + \tau_{ij})}{\partial x_j},$$

with continuity:

$$\frac{\partial U_i}{\partial x_i} = 0,$$

$$\tau_{ij} = 2\mu_t S_{ij} - \frac{2}{3}\rho k \delta_{ij},$$

Boussinesq's hypothesis

□ Five turbulence models are used:

1. Reynolds stress turbulence model
  - 1.1. Linear pressure-strain model (LRST)
  - 1.2. Quadratic pressure-strain model (QRST)
  - 1.3. Elliptic blending pressure-strain model (ERST)
2. SST k-w turbulence model
  - 2.1. Linear eddy viscosity SST k-w
  - 2.2. Quadratic nonlinear SST k-w

F. R. Menter (1994), J. Boussinesq (1877)



**COPPE**  
Instituto Alberto Luiz Coimbra de  
Pós-Graduação e Pesquisa de Engenharia



**GERO**



**CNPq**  
Conselho Nacional de Desenvolvimento  
Científico e Tecnológico

# Numerical Model:

□ STARCCM+ is used.

□ Modeling the fluid flow:

$$\frac{\partial(\rho U_i)}{\partial t} + \frac{\partial(\rho U_j U_i)}{\partial x_j} = -\frac{\partial P}{\partial x_i} + \frac{\partial(2\mu S_{ij} + \tau_{ij})}{\partial x_j},$$

with continuity:

$$\frac{\partial U_i}{\partial x_i} = 0,$$

$$\tau_{ij} = 2\mu_t S_{ij} - \frac{2}{3}\rho k \delta_{ij},$$

□ Five turbulence models are used:

1. Reynolds stress turbulence model
  - 1.1. Linear pressure-strain model (LRST)
  - 1.2. Quadratic pressure-strain model (QRST)
  - 1.3. Elliptic blending pressure-strain model (ERST)
2. SST k-w turbulence model
  - 2.1. Linear eddy viscosity SST k-w
  - 2.2. Quadratic nonlinear SST k-w

An alignment between the Reynolds stresses and the mean deformation rate of the flow.

$$\gamma_\tau = \text{atan} \left\{ \frac{\tau_{23}}{\tau_{12}} \right\}, \quad \gamma_g = \text{atan} \left\{ \frac{\frac{\partial U_2}{\partial x_3} + \frac{\partial U_3}{\partial x_2}}{\frac{\partial U_1}{\partial x_2} + \frac{\partial U_2}{\partial x_1}} \right\},$$

F. R. Menter (1994), J. Boussinesq (1877)



# Numerical Model:

□ STARCCM+ is used.

□ Modeling the fluid flow:

$$\frac{\partial(\rho U_i)}{\partial t} + \frac{\partial(\rho U_j U_i)}{\partial x_j} = -\frac{\partial P}{\partial x_i} + \frac{\partial(2\mu S_{ij} + \tau_{ij})}{\partial x_j},$$

with continuity:

$$\frac{\partial U_i}{\partial x_i} = 0,$$

$$\tau_{ij} = 2\mu_t S_{ij} - \frac{2}{3}\rho k \delta_{ij} - 2 \times 0.04645 \mu_t (O_{ij} \cdot S_{ij} - S_{ij} \cdot O_{ij}),$$

$$O_{ij} = \frac{\Omega_{ij}}{\sqrt{(S_{ij} - \Omega_{ij})(S_{ij} + \Omega_{ij})}},$$

□ Five turbulence models are used:

1. Reynolds stress turbulence model
  - 1.1. Linear pressure-strain model (LRST)
  - 1.2. Quadratic pressure-strain model (QRST)
  - 1.3. Elliptic blending pressure-strain model (ERST)
2. SST k-w turbulence model
  - 2.1. Linear eddy viscosity SST k-w
  - 2.2. Quadratic nonlinear SST k-w

F. R. Menter (1994), J. Boussinesq (1877). P. Durbin (1996), S. K. Arolla, P. A. Durbin (2013)



# Numerical Model:

□ STARCCM+ is used.

□ Modeling the fluid flow:

$$\frac{\partial(\rho U_i)}{\partial t} + \frac{\partial(\rho U_j U_i)}{\partial x_j} = -\frac{\partial P}{\partial x_i} + \frac{\partial(2\mu S_{ij} + \tau_{ij})}{\partial x_j},$$

with continuity:

$$\frac{\partial U_i}{\partial x_i} = 0,$$

$$\frac{\partial(\tau_{ij})}{\partial t} + \nabla \cdot (\tau_{ij} \cdot U) = \nabla \cdot \left[ \mu + \frac{\mu_t}{\sigma_k} \right] \frac{\nabla \tau_{ij}}{\rho} + P_{ij} - \frac{2}{3} \varepsilon \mathbf{I} + \Pi_{ij},$$

$$\frac{\partial(\rho \varepsilon)}{\partial t} + \nabla \cdot (\rho \varepsilon U) =$$

$$\nabla \cdot \left[ \mu + \mu_t \sigma_k \right] \nabla \varepsilon + \frac{\varepsilon}{k} \left[ C_{\varepsilon 1} \left( \frac{1}{2} \text{tr}(P_{ij}) \right) - C_{\varepsilon 2} \rho \varepsilon \right],$$

□ Five turbulence models are used:

1. Reynolds stress turbulence model
  - 1.1. Linear pressure-strain model (LRST)
  - 1.2. Quadratic pressure-strain model (QRST)
  - 1.3. Elliptic blending pressure-strain model (ERST)
2. SST k-w turbulence model
  - 2.1. Linear eddy viscosity SST k-w
  - 2.2. Quadratic nonlinear SST k-w

STARCCM+ (2017)



**COPPE**  
Instituto Alberto Luiz Coimbra de  
Pós-Graduação e Pesquisa de Engenharia



# Numerical Model:

□ STARCCM+ is used.

□ Modeling the fluid flow:

$$\frac{\partial(\rho U_i)}{\partial t} + \frac{\partial(\rho U_j U_i)}{\partial x_j} = -\frac{\partial P}{\partial x_i} + \frac{\partial(2\mu S_{ij} + \tau_{ij})}{\partial x_j},$$

with continuity:

$$\frac{\partial U_i}{\partial x_i} = 0,$$

□ Five turbulence models are used:

1. Reynolds stress turbulence model
  - 1.1. Linear pressure-strain model (LRST)
  - 1.2. Quadratic pressure-strain model (QRST)
  - 1.3. Elliptic blending pressure-strain model (ERST)
2. SST k-w turbulence model
  - 2.1. Linear eddy viscosity SST k-w
  - 2.2. Quadratic nonlinear SST k-w

$$\frac{\partial(\tau_{ij})}{\partial t} + \nabla \cdot (\tau_{ij} \cdot U) = \nabla \cdot \left[ \mu + \frac{\mu_t}{\sigma_k} \right] \frac{\nabla \tau_{ij}}{\rho} + P_{ij} - \frac{2}{3} \varepsilon \mathbf{I} + \Pi_{ij}, \quad \text{turbulent pressure-strain interaction}$$

$$\frac{\partial(\rho \varepsilon)}{\partial t} + \nabla \cdot (\rho \varepsilon U) = \nabla \cdot [\mu + \mu_t \sigma_k] \nabla \varepsilon + \frac{\varepsilon}{k} \left[ C_{\varepsilon 1} \left( \frac{1}{2} \text{tr}(P_{ij}) \right) - C_{\varepsilon 2} \rho \varepsilon \right],$$

STARCCM+ (2017)

# Numerical Model:

□ STARCCM+ is used.

□ Modeling the fluid flow:

$$\frac{\partial(\rho U_i)}{\partial t} + \frac{\partial(\rho U_j U_i)}{\partial x_j} = -\frac{\partial P}{\partial x_i} + \frac{\partial(2\mu S_{ij} + \tau_{ij})}{\partial x_j},$$

with continuity:

$$\frac{\partial U_i}{\partial x_i} = 0,$$

$$\frac{\partial(\tau_{ij})}{\partial t} + \nabla \cdot (\tau_{ij} \cdot U) = \nabla \cdot \left[ \mu + \frac{\mu_t}{\sigma_k} \right] \frac{\nabla \tau_{ij}}{\rho} + P_{ij} - \frac{2}{3} \varepsilon \mathbf{I} + \Pi_{ij},$$

$$\Pi = \Pi_s + \Pi_r + \Pi_w.$$

□ Five turbulence models are used:

1. Reynolds stress turbulence model

1.1. Linear pressure-strain model (LRST)

1.2. Quadratic pressure-strain model (QRST)

1.3. Elliptic blending pressure-strain model (ERST)

2. SST k-w turbulence model

2.1. Linear eddy viscosity SST k-w

2.2. Quadratic nonlinear SST k-w

STARCCM+ (2017), B. E. Launder, N. Shima (1989)



# Numerical Model:

□ STARCCM+ is used.

□ Modeling the fluid flow:

$$\frac{\partial(\rho U_i)}{\partial t} + \frac{\partial(\rho U_j U_i)}{\partial x_j} = -\frac{\partial P}{\partial x_i} + \frac{\partial(2\mu S_{ij} + \tau_{ij})}{\partial x_j},$$

with continuity:

$$\frac{\partial U_i}{\partial x_i} = 0,$$

$$\frac{\partial(\tau_{ij})}{\partial t} + \nabla \cdot (\tau_{ij} \cdot U) = \nabla \cdot \left[ \mu + \frac{\mu_t}{\sigma_k} \right] \frac{\nabla \tau_{ij}}{\rho} + P_{ij} - \frac{2}{3} \varepsilon \mathbf{I} + \Pi_{ij},$$

□ Five turbulence models are used:

1. Reynolds stress turbulence model

1.1. Linear pressure-strain model (LRST)

1.2. Quadratic pressure-strain model (QRST)

1.3. Elliptic blending pressure-strain model (ERST)

2. SST k-w turbulence model

2.1. Linear eddy viscosity SST k-w

2.2. Quadratic nonlinear SST k-w

$$\begin{aligned} \Pi_{ij} = & - [C_{s1}\rho\varepsilon + C_{r4}tr(P)] A_{ij} \\ & + C_{s2}\rho\varepsilon \left( A_{ik}A_{kj} - \frac{1}{3}A_{mn}A_{mn}\delta_{ij} \right) + \\ & (C_{r3} - C_{r3}^* \sqrt{A_{ij}A_{ij}}) \rho k S_{ij} + \\ & C_{r1}\rho k \left( A_{ik}S_{jk} + S_{ik}A_{jk} - \frac{2}{3}A_{mn}S_{mn}\delta_{ij} \right) \\ & + C_{r2}\rho k \left( A_{ik}\Omega_{jk} + \Omega_{ik}A_{jk} \right), \end{aligned}$$

STARCCM+ (2017), B. E. Launder, N. Shima (1989), C. G. Speziale et al. (1991)





# Numerical Model:

□ STARCCM+ is used.

□ Modeling the fluid flow:

$$\frac{\partial(\rho U_i)}{\partial t} + \frac{\partial(\rho U_j U_i)}{\partial x_j} = -\frac{\partial P}{\partial x_i} + \frac{\partial(2\mu S_{ij} + \tau_{ij})}{\partial x_j},$$

with continuity:

$$\frac{\partial U_i}{\partial x_i} = 0,$$

$$\frac{\partial(\tau_{ij})}{\partial t} + \nabla \cdot (\tau_{ij} \cdot U) = \nabla \cdot \left[ \mu + \frac{\mu_t}{\sigma_k} \right] \frac{\nabla \tau_{ij}}{\rho} + P_{ij} - \frac{2}{3} \varepsilon \mathbf{I} + \Pi_{ij},$$

Anisotropy Tensor

□ Five turbulence models are used:

1. Reynolds stress turbulence model

1.1. Linear pressure-strain model (LRST)

1.2. Quadratic pressure-strain model (QRST)

1.3. Elliptic blending pressure-strain model (ERST)

2. SST k-w turbulence model

2.1. Linear eddy viscosity SST k-w

2.2. Quadratic nonlinear SST k-w

$$\begin{aligned} \Pi_{ij} = & - [C_{s1}\rho\varepsilon + C_{r4}tr(P)] A_{ij} \\ & + C_{s2}\rho\varepsilon \left( A_{ik}A_{kj} - \frac{1}{3}A_{mn}A_{mn}\delta_{ij} \right) + \\ & (C_{r3} - C_{r3}^* \sqrt{A_{ij}A_{ij}}) \rho k S_{ij} + \\ & C_{r1}\rho k \left( A_{ik}S_{jk} + S_{ik}A_{jk} - \frac{2}{3}A_{mn}S_{mn}\delta_{ij} \right) \\ & + C_{r2}\rho k \left( A_{ik}\Omega_{jk} + \Omega_{ik}A_{jk} \right), \end{aligned}$$

STARCCM+ (2017), B. E. Launder, N. Shima (1989), C. G. Speziale et al. (1991)

# Numerical Model:

□ STARCCM+ is used.

□ Modeling the fluid flow:

$$\frac{\partial(\rho U_i)}{\partial t} + \frac{\partial(\rho U_j U_i)}{\partial x_j} = -\frac{\partial P}{\partial x_i} + \frac{\partial(2\mu S_{ij} + \tau_{ij})}{\partial x_j},$$

with continuity:

$$\frac{\partial U_i}{\partial x_i} = 0,$$

$$\frac{\partial(\tau_{ij})}{\partial t} + \nabla \cdot (\tau_{ij} \cdot U) = \nabla \cdot \left[ \mu + \frac{\mu_t}{\sigma_k} \right] \frac{\nabla \tau_{ij}}{\rho} + P_{ij} - \frac{2}{3} \varepsilon \mathbf{I} + \Pi_{ij},$$

$$\Pi - \varepsilon = (1 - \alpha^3)(\Pi^w - \varepsilon^w) + \alpha^3(\Pi^h - \varepsilon^h)$$

blending parameter

□ Five turbulence models are used:

1. Reynolds stress turbulence model

1.1. Linear pressure-strain model (LRST)

1.2. Quadratic pressure-strain model (QRST)

1.3. Elliptic blending pressure-strain model (ERST)

2. SST k-w turbulence model

2.1. Linear eddy viscosity SST k-w

2.2. Quadratic nonlinear SST k-w

STARCCM+ (2017), B. E. Launder, N. Shima (1989), C. G. Speziale et al. (1991), P. Durbin, (1993), S. Lardeau, R. Manceau (2014)



# Numerical Model:

□ STARCCM+ is used.

□ Modeling the fluid flow:

$$\frac{\partial(\rho U_i)}{\partial t} + \frac{\partial(\rho U_j U_i)}{\partial x_j} = -\frac{\partial P}{\partial x_i} + \frac{\partial(2\mu S_{ij} + \tau_{ij})}{\partial x_j},$$

with continuity:

$$\frac{\partial U_i}{\partial x_i} = 0,$$

$$\frac{\partial(\tau_{ij})}{\partial t} + \nabla \cdot (\tau_{ij} \cdot U) = \nabla \cdot \left[ \mu + \frac{\mu_t}{\sigma_k} \right] \frac{\nabla \tau_{ij}}{\rho} + P_{ij} - \frac{2}{3} \varepsilon \mathbf{I} + \Pi_{ij},$$

$$\Pi - \varepsilon = (1 - \alpha^3)(\Pi^w - \varepsilon^w) + \alpha^3(\Pi^h - \varepsilon^h)$$

blending parameter

□ Five turbulence models are used:

1. Reynolds stress turbulence model

1.1. Linear pressure-strain model (LRST)

1.2. Quadratic pressure-strain model (QRST)

1.3. Elliptic blending pressure-strain model (ERST)

2. SST k-w turbulence model

$$2.1 \quad \Pi^h_{ij} = -[C_1 \rho \varepsilon + C_{1s} tr(P)] A_{ij}$$

$$2.2 \quad + (C_3 - C_{3s} \sqrt{A_{ij} A_{ij}}) \rho k S_{ij}$$

$$+ C_4 \rho k \left( A_{ik} S_{jk} + S_{ik} A_{jk} - \frac{2}{3} A_{mn} S_{mn} \delta_{ij} \right) +$$

$$C_5 \rho k (A_{ik} \Omega_{jk} + \Omega_{ik} A_{jk}).$$

$$\Pi^w_{ij} = 5 \frac{\varepsilon}{k} \left[ \frac{\tau_{ik}}{\rho} n_j n_k + \frac{\tau_{jk}}{\rho} n_i n_k - \frac{1}{2} \frac{\tau_{kl}}{\rho} n_k n_l (n_i n_j + \delta_{ij}) \right]$$

STARCCM+ (2017), B. E. Launder, N. Shima (1989), C. G. Speziale et al. (1991), P. Durbin, (1993), S. Lardeau, R. Manceau (2014)



# Numerical Model:

- ❑ STARCCM+ is used.
- ❑ Modeling the fluid flow:

$$\frac{\partial(\rho U_i)}{\partial t} + \frac{\partial(\rho U_j U_i)}{\partial x_j} = -\frac{\partial P}{\partial x_i} + \frac{\partial(2\mu S_{ij} + \tau_{ij})}{\partial x_j},$$

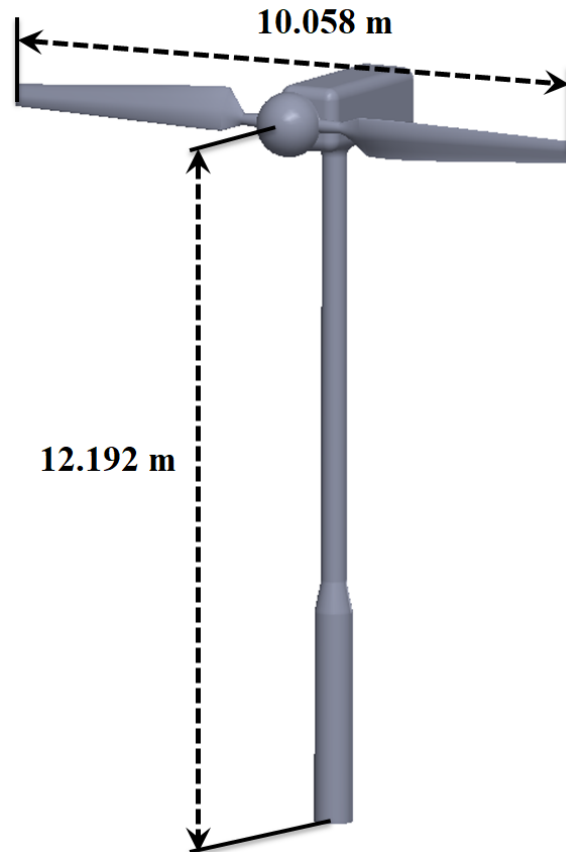
with continuity:

$$\frac{\partial U_i}{\partial x_i} = 0,$$

- ❑ Discretization schemes:
  - Second-order schemes for convective and diffusion terms.
  - Second-order implicit scheme for transient term.
- ❑ A SIMPLE-type solver is used for pressure-velocity coupling
- ❑ The simulations are performed for four rotor revolutions.

# Geometry and Computational Conditions:

- The NREL phase VI horizontal axis wind turbine

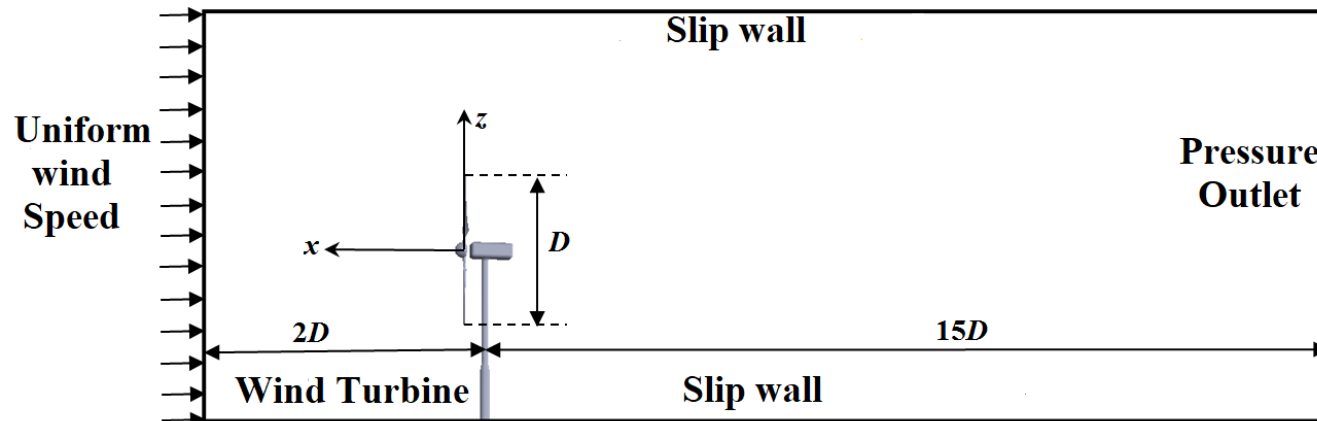
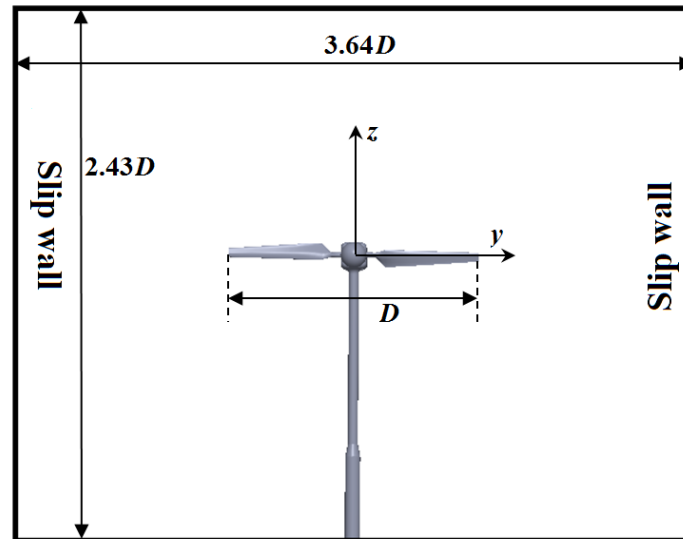


## Computational Conditions:

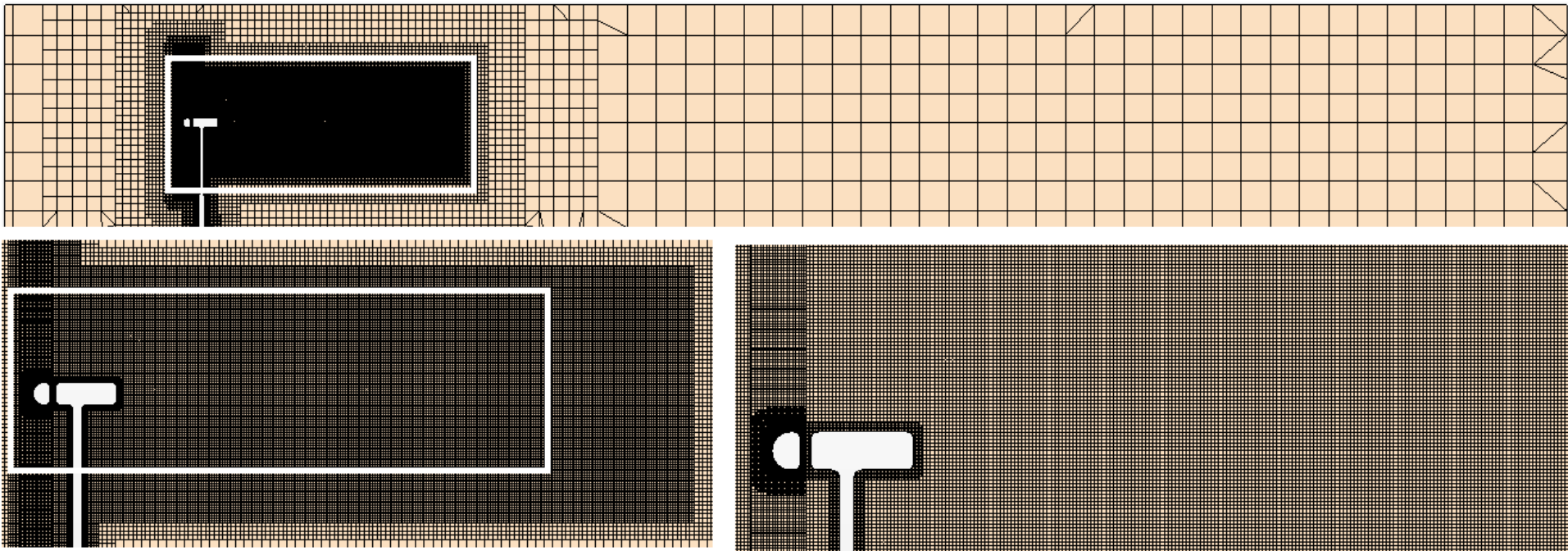
1. Four wind speeds: 5, 10, 15 and 25 m/s
2. Rotor angular velocity: 72 rpm
3. Turbulence intensity: 0.5%

P. Giguere, M. Selig (1999), M. Hand et al. (2001)

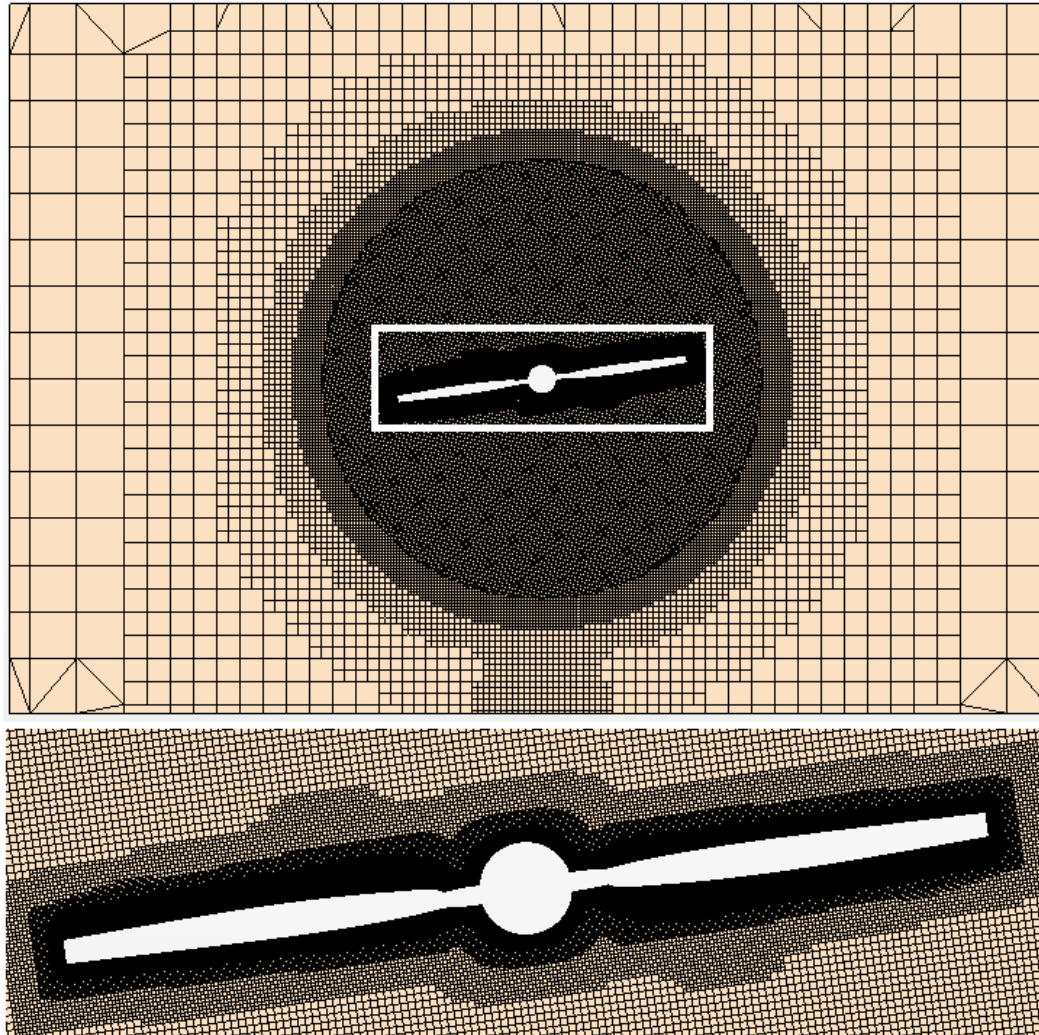
# Computational Domain and Boundary Conditions:



Grid:

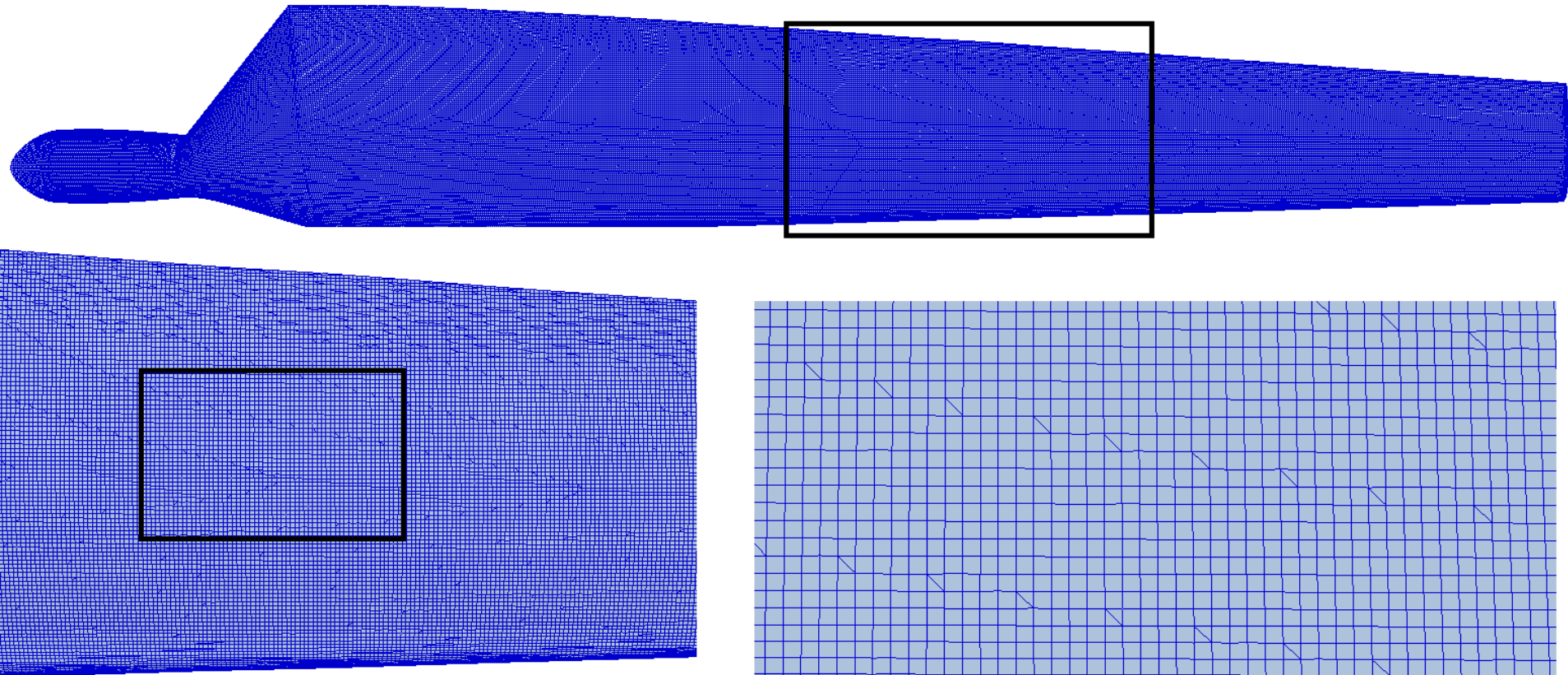


Grid:





Grid:



# Grid convergence study:

Richardson (1911), Richards (1997), Stern et al. (2006), Mchale and Friedman (2009).

# Grid convergence study:

Wind Speed: 25 m/s

Turbulence model: nonlinear quadratic SST k-w model

# Grid convergence study:

Wind Speed: 25 m/s

Turbulence model: nonlinear quadratic SST k-w model

Grid	Grid Refinement	Time step (s)	# of cells
<i>I</i>	Fine	0.001155/1.2	26,806,032
<i>II</i>	Medium	0.001155	17,345,028
<i>III</i>	Coarse	0.001155 × 1.2	11,362,711

# Grid convergence study:

Wind Speed: 25 m/s

Turbulence model: nonlinear quadratic SST k-w model

Grid	Grid Refinement	Time step (s)	# of cells
<i>I</i>	Fine	0.001155/1.2	26,806,032
<i>II</i>	Medium	0.001155	17,345,028
<i>III</i>	Coarse	0.001155 × 1.2	11,362,711

Grid	Power (W)	Thrust (N)
<i>I</i>	12574.13	3927.126
<i>II</i>	12108.03	3912.806
<i>III</i>	11150.63	3888.066

Grid convergence study:  $R_G = \frac{S_I - S_{II}}{S_{II} - S_{III}}$  ,  $U_G = 1.25 \left| \frac{S_I - S_{II}}{S_{II}(r_{12}^p - 1)} \right|$  .

Wind Speed: 25 m/s

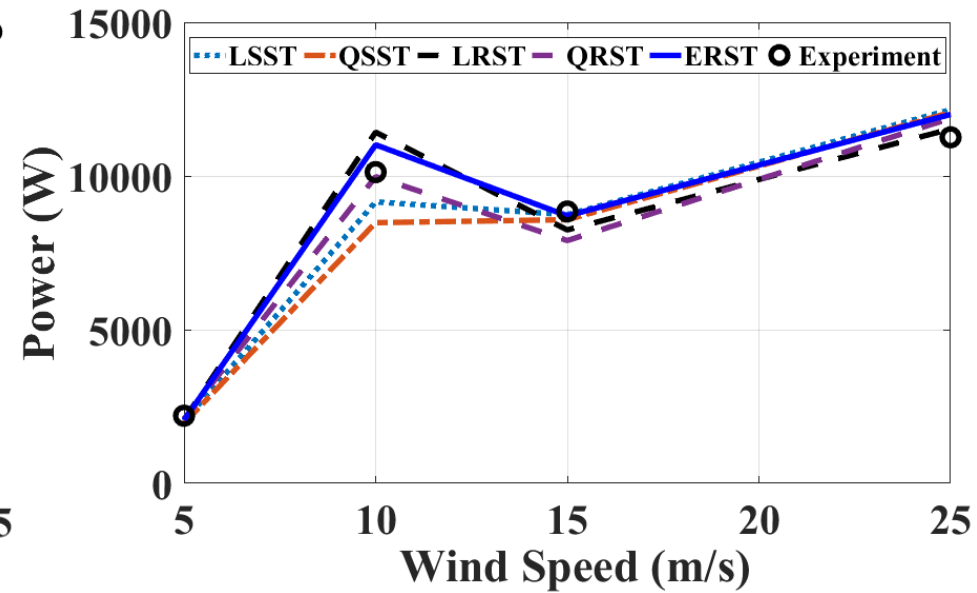
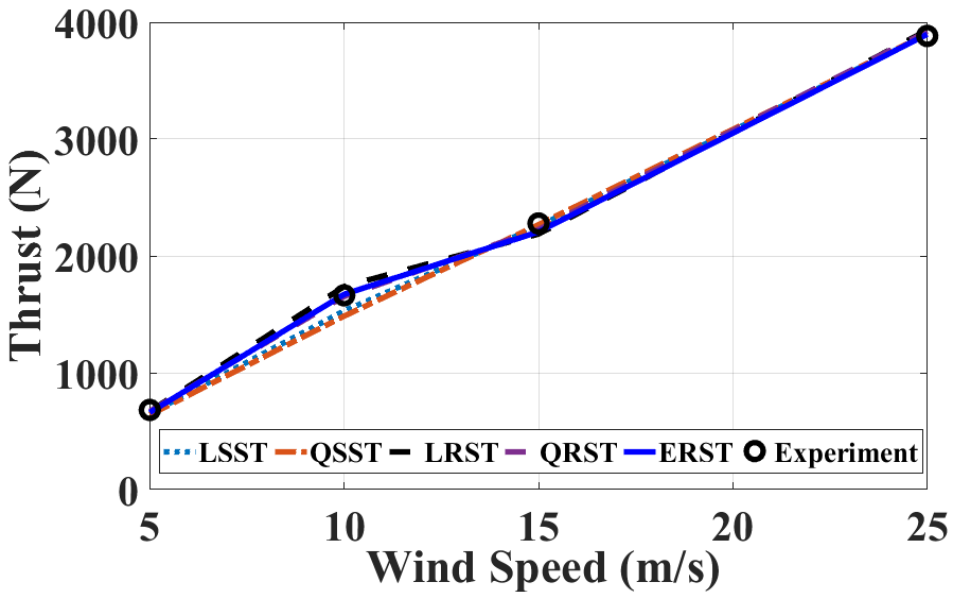
Turbulence model: nonlinear quadratic SST k-w model

Grid	Grid Refinement	Time step (s)	# of cells
<i>I</i>	Fine	0.001155/1.2	26,806,032
<i>II</i>	Medium	0.001155	17,345,028
<i>III</i>	Coarse	0.001155 × 1.2	11,362,711

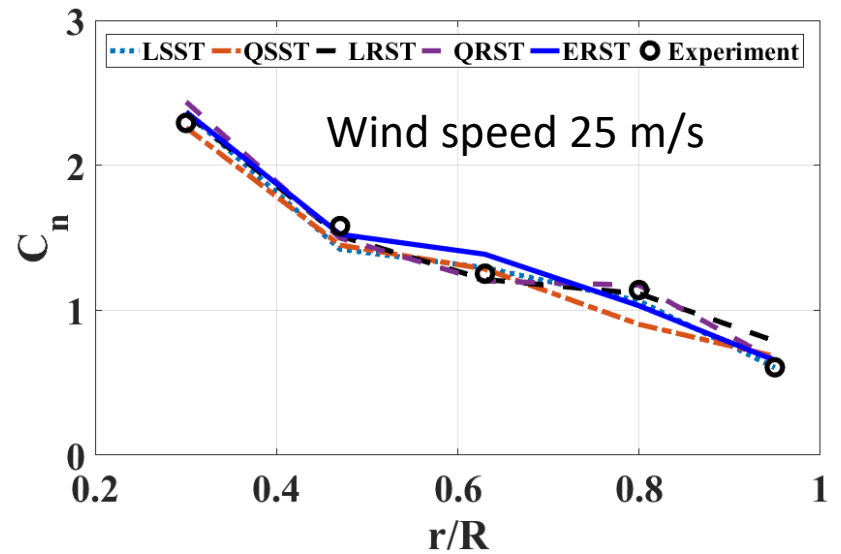
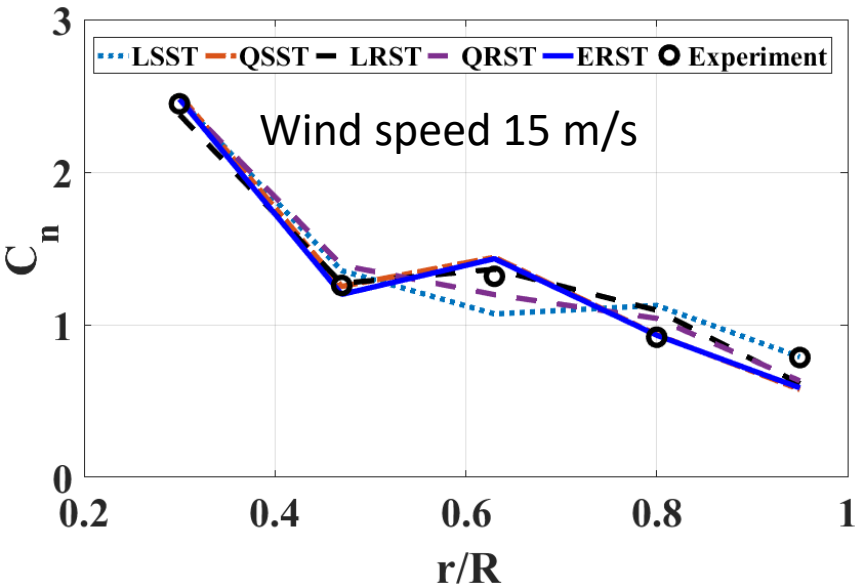
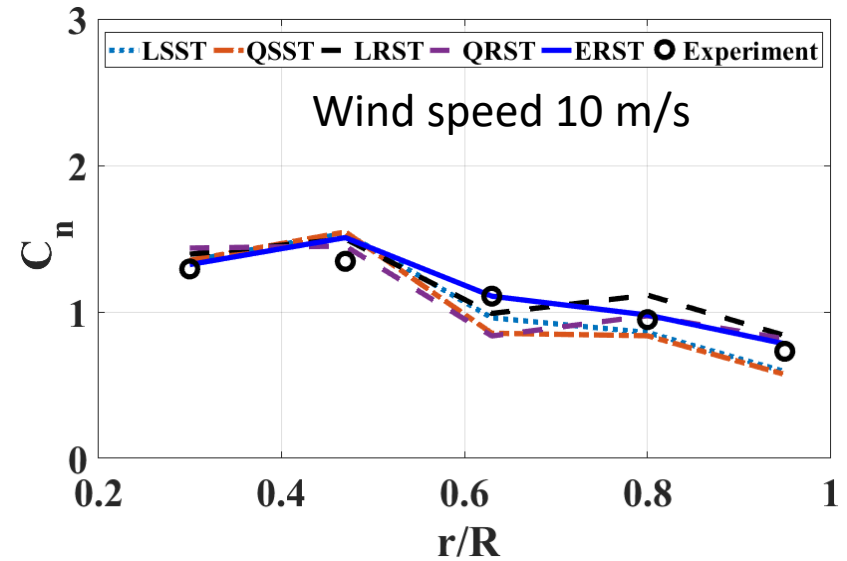
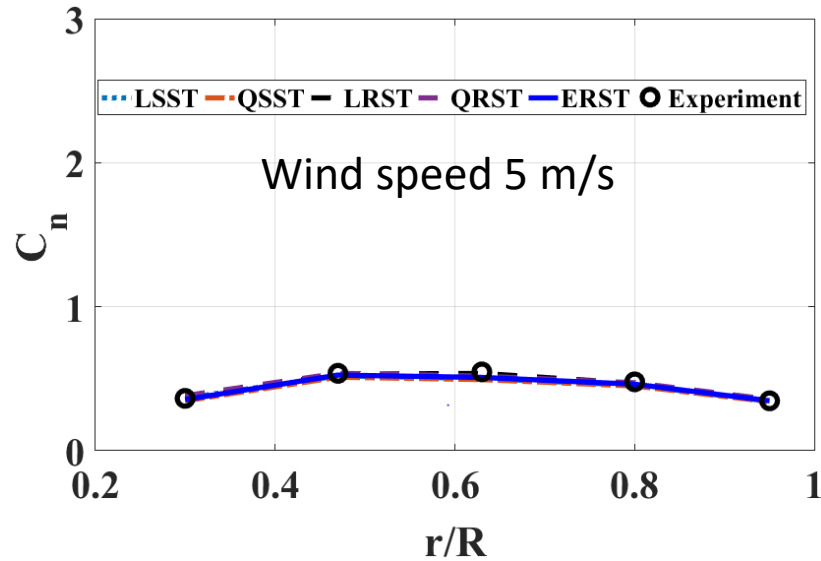
Grid	Power (W)	Thrust (N)
<i>I</i>	12574.13	3927.126
<i>II</i>	12108.03	3912.806
<i>III</i>	11150.63	3888.066

Quantity	$R_G$	$p$	$U_G \% S_{II}$
Power	0.49	4.99	4.52
Thrust	0.58	4.03	0.58

# Thrust and Power



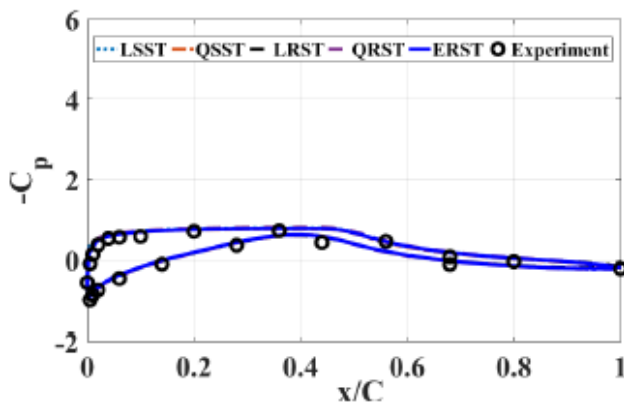
# Radial distribution of normal force coefficient



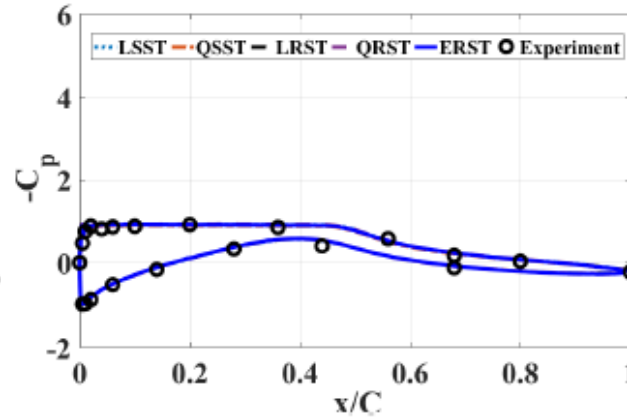


# Chordwise pressure coefficient distribution

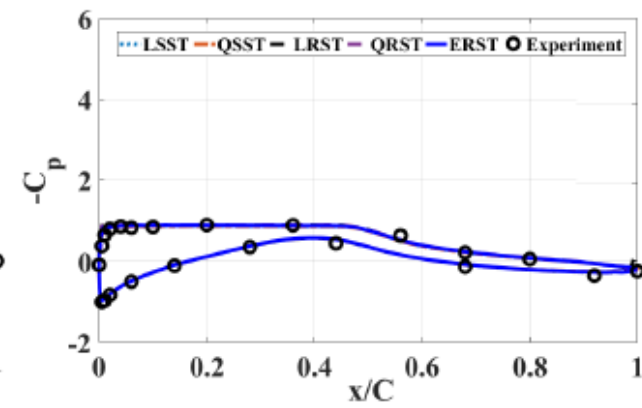
Wind speed 5 m/s



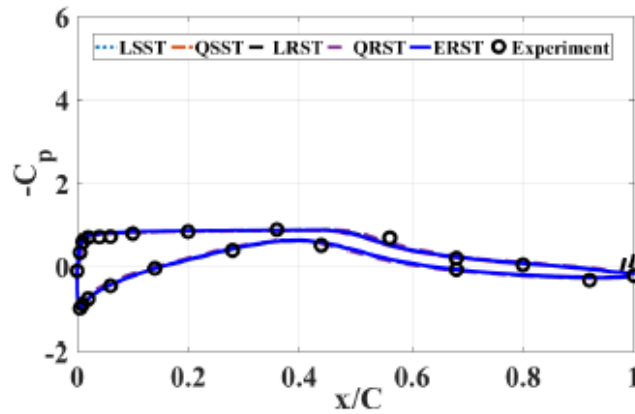
(a)  $r/R = 0.30$



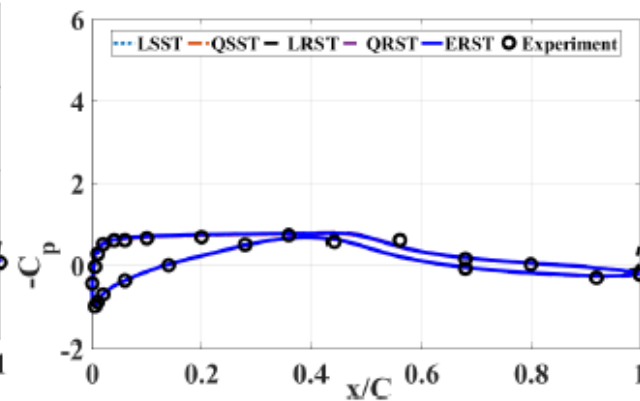
(b)  $r/R = 0.47$



(c)  $r/R = 0.63$



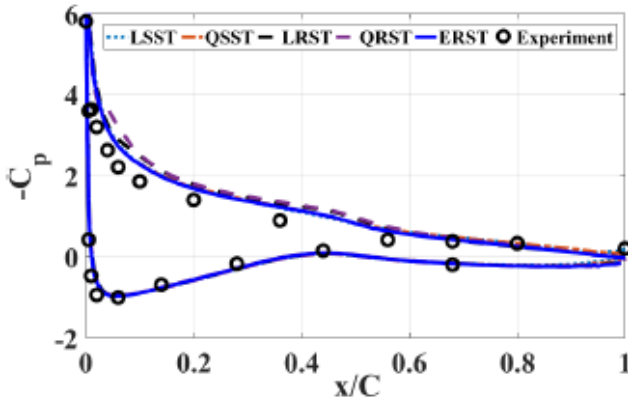
(d)  $r/R = 0.80$



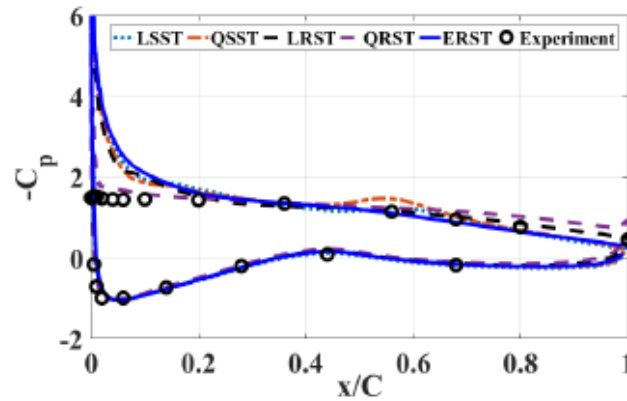
(e)  $r/R = 0.95$

# Chordwise pressure coefficient distribution

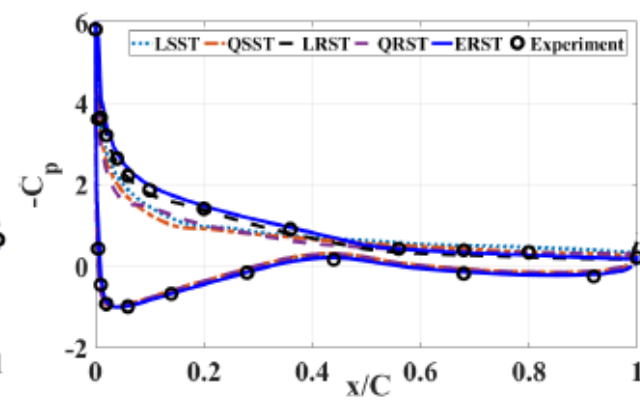
Wind speed 10 m/s



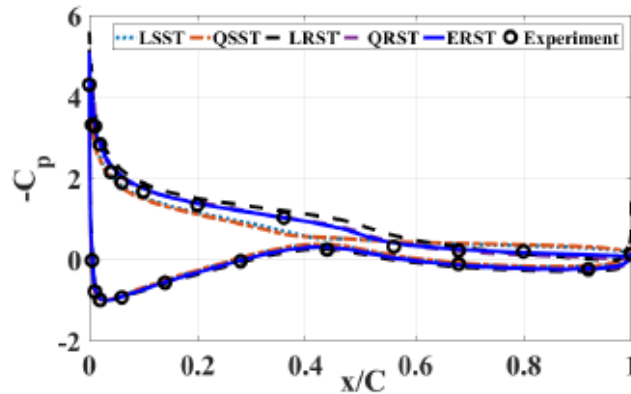
(a)  $r/R = 0.30$



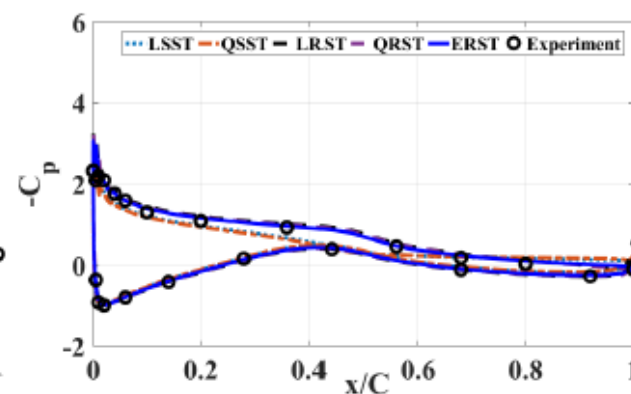
(b)  $r/R = 0.47$



(c)  $r/R = 0.63$



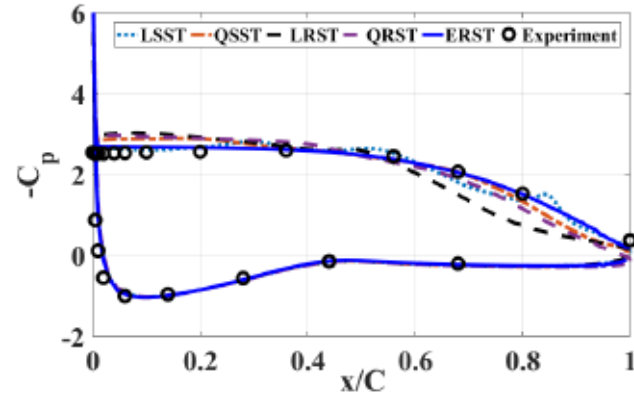
(d)  $r/R = 0.80$



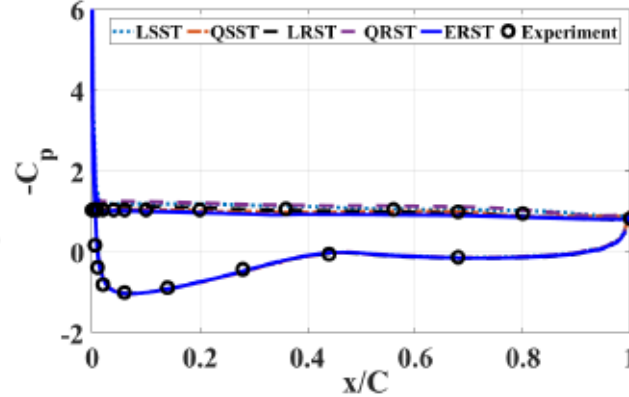
(e)  $r/R = 0.95$

# Chordwise pressure coefficient distribution

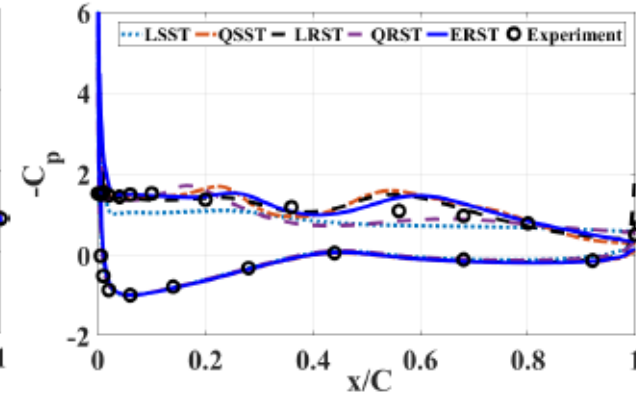
Wind speed 15 m/s



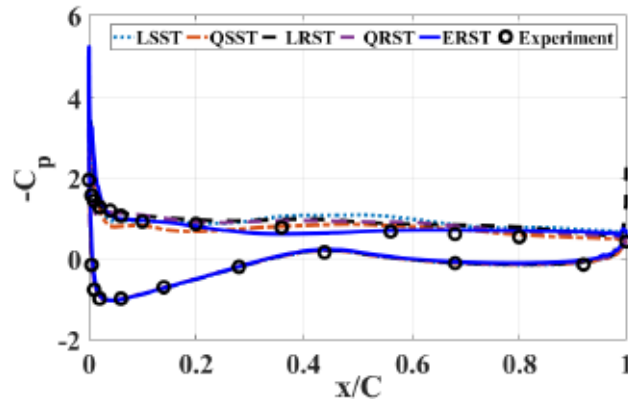
(a)  $r/R = 0.30$



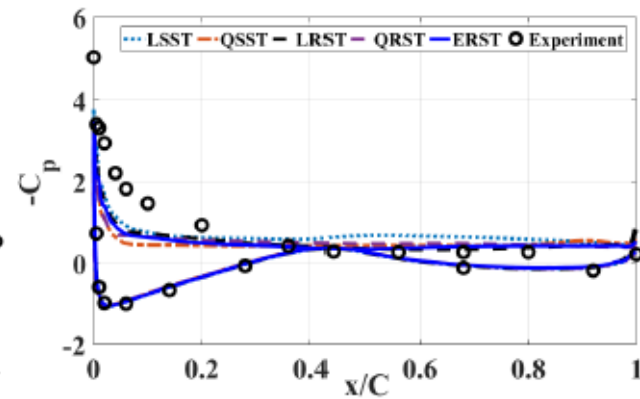
(b)  $r/R = 0.47$



(c)  $r/R = 0.63$



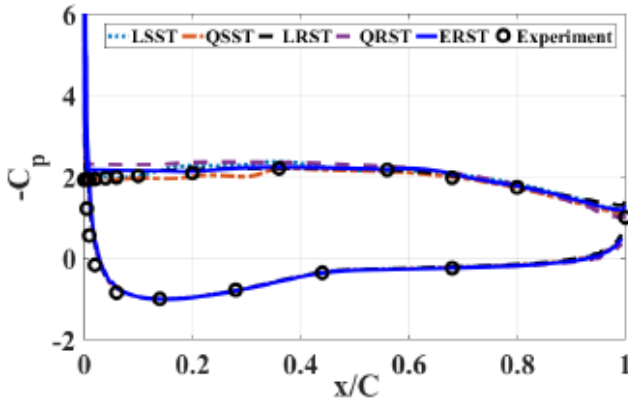
(d)  $r/R = 0.80$



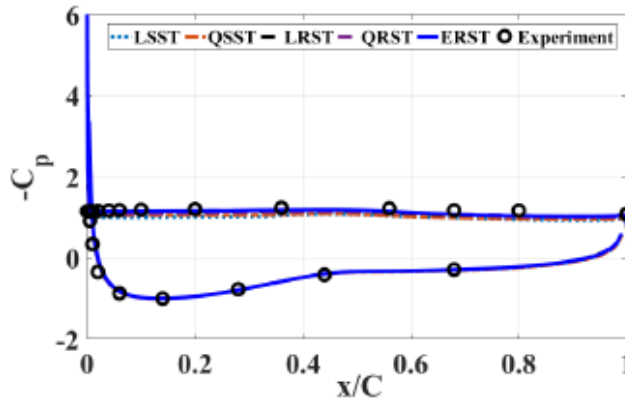
(e)  $r/R = 0.95$

# Chordwise pressure coefficient distribution

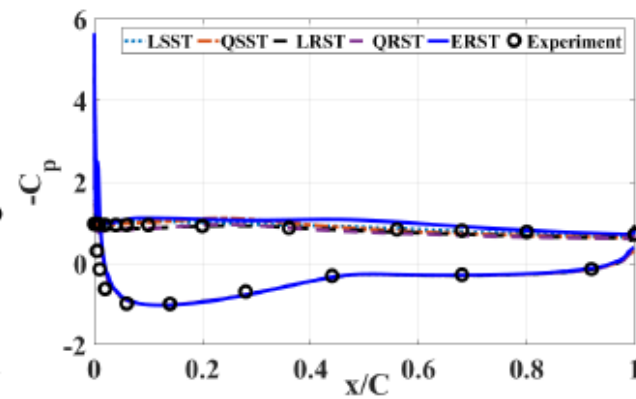
Wind speed 25 m/s



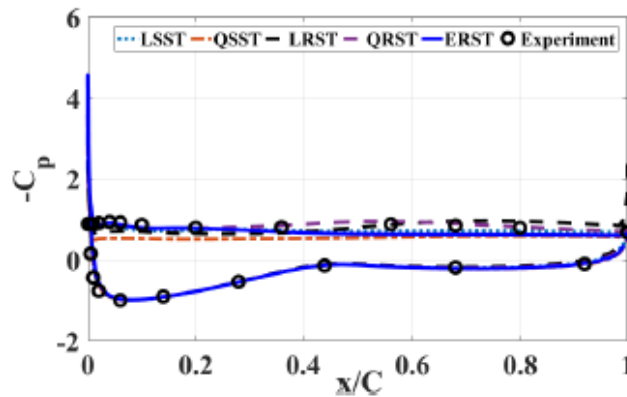
(a)  $r/R = 0.30$



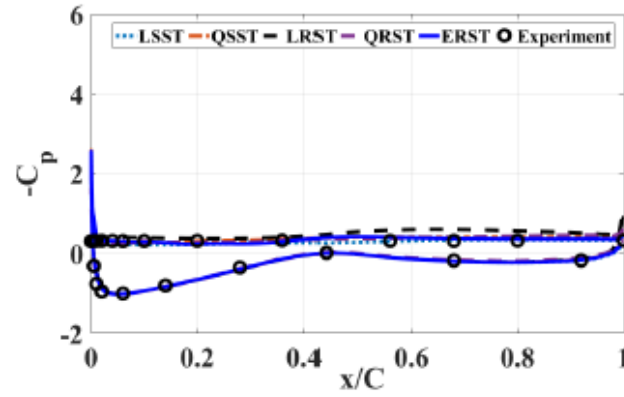
(b)  $r/R = 0.47$



(c)  $r/R = 0.63$



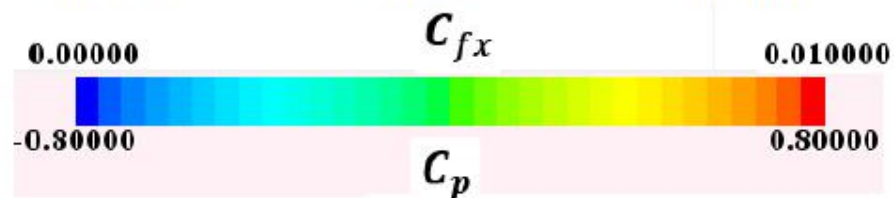
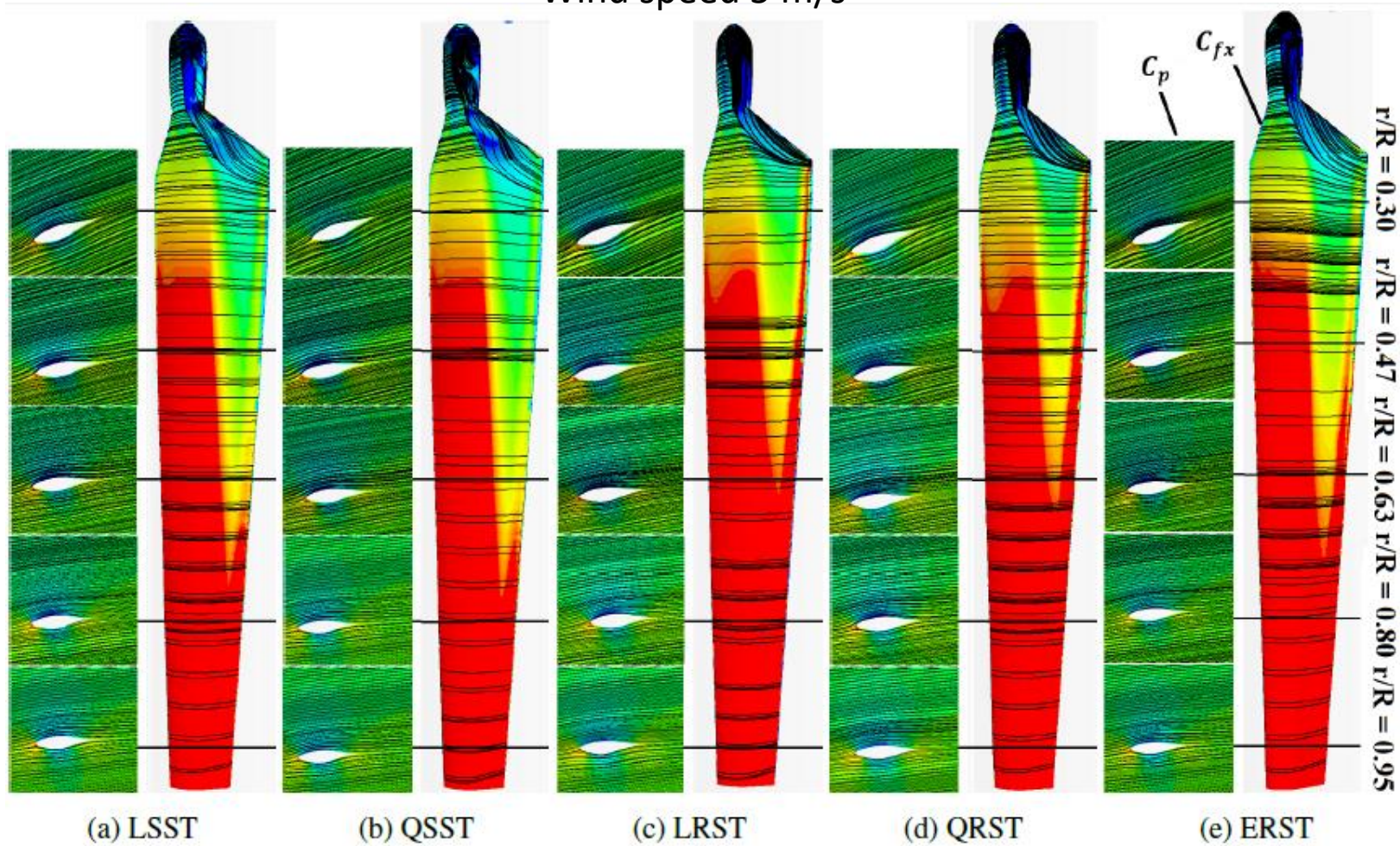
(d)  $r/R = 0.80$



(e)  $r/R = 0.95$

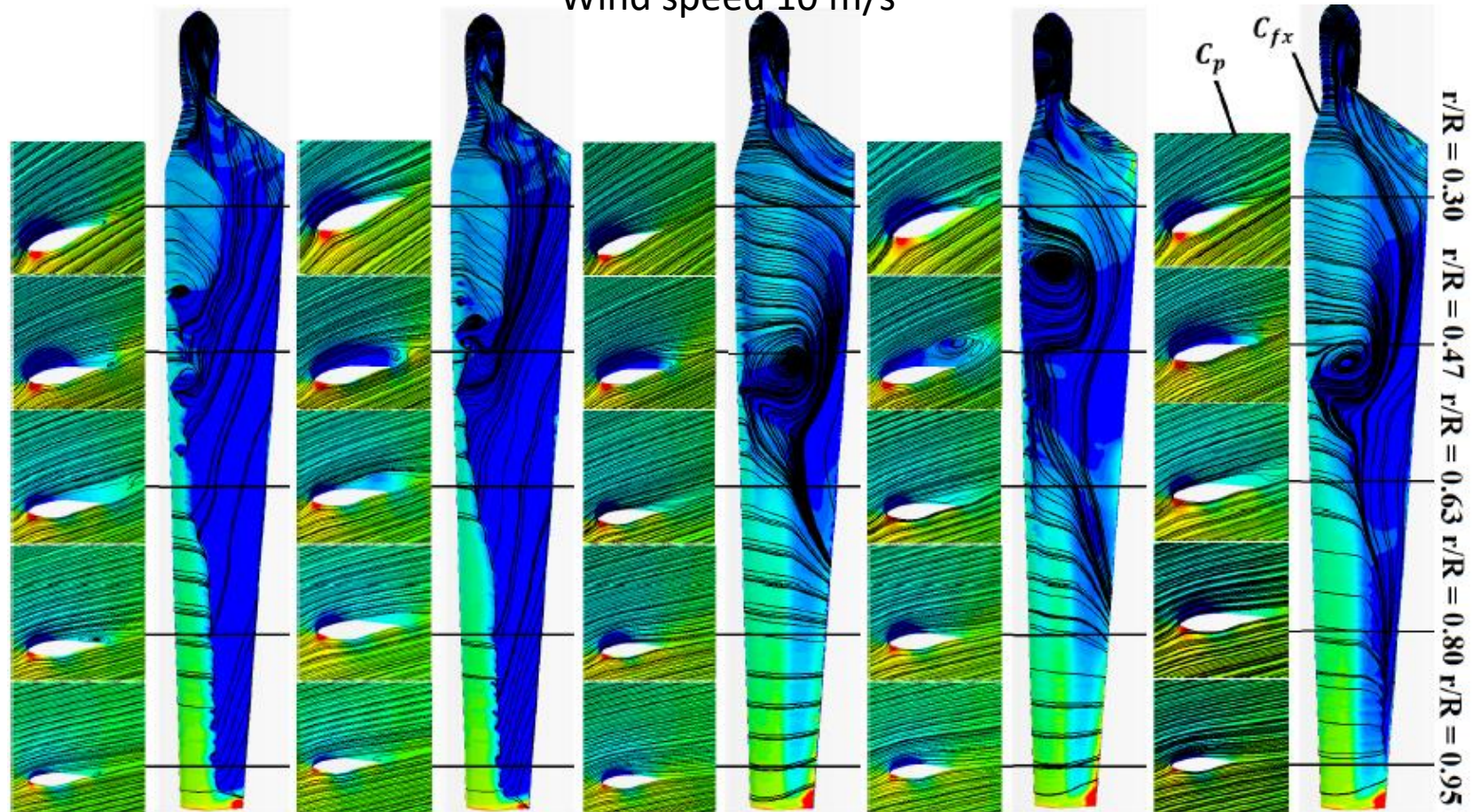
## Flow visualization

Wind speed 5 m/s



## Flow visualization

Wind speed 10 m/s



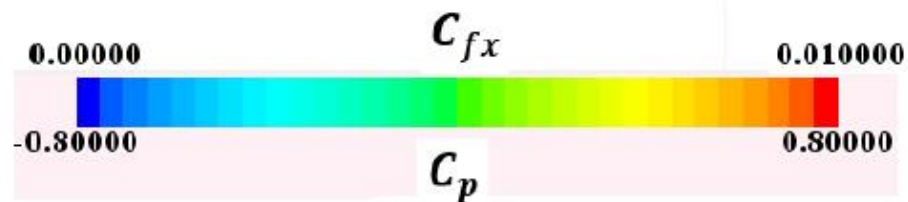
(a) LSST

(b) QSST

(c) LRST

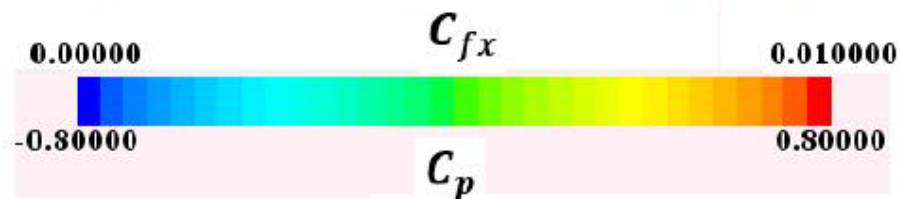
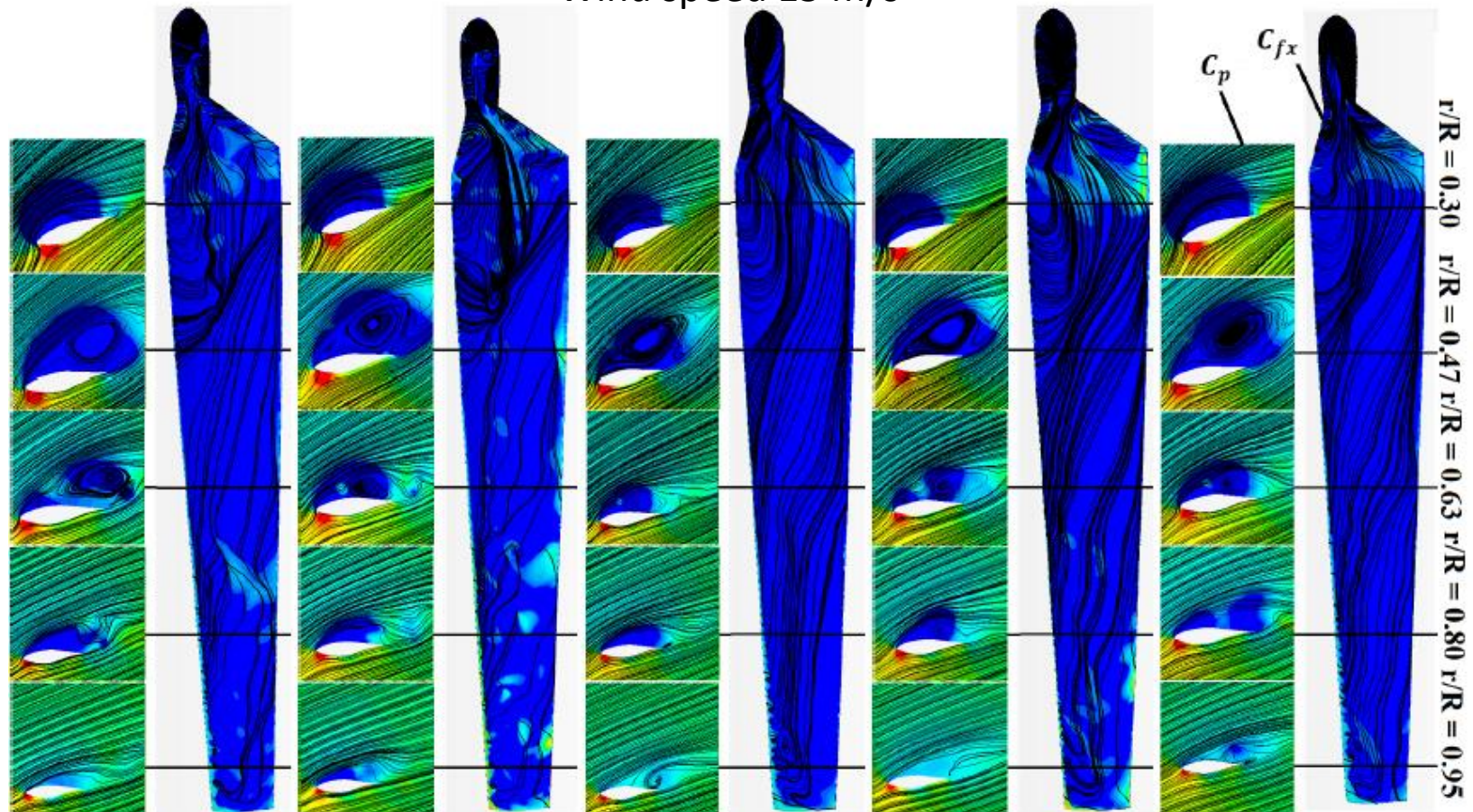
(d) QRST

(e) ERST



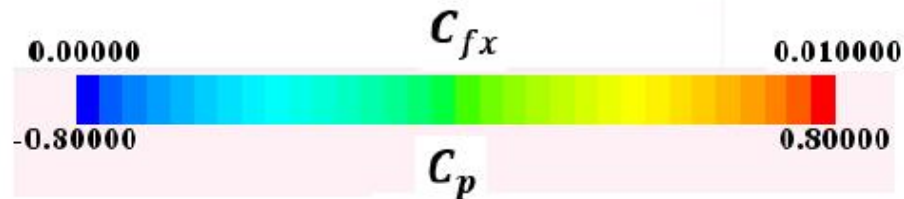
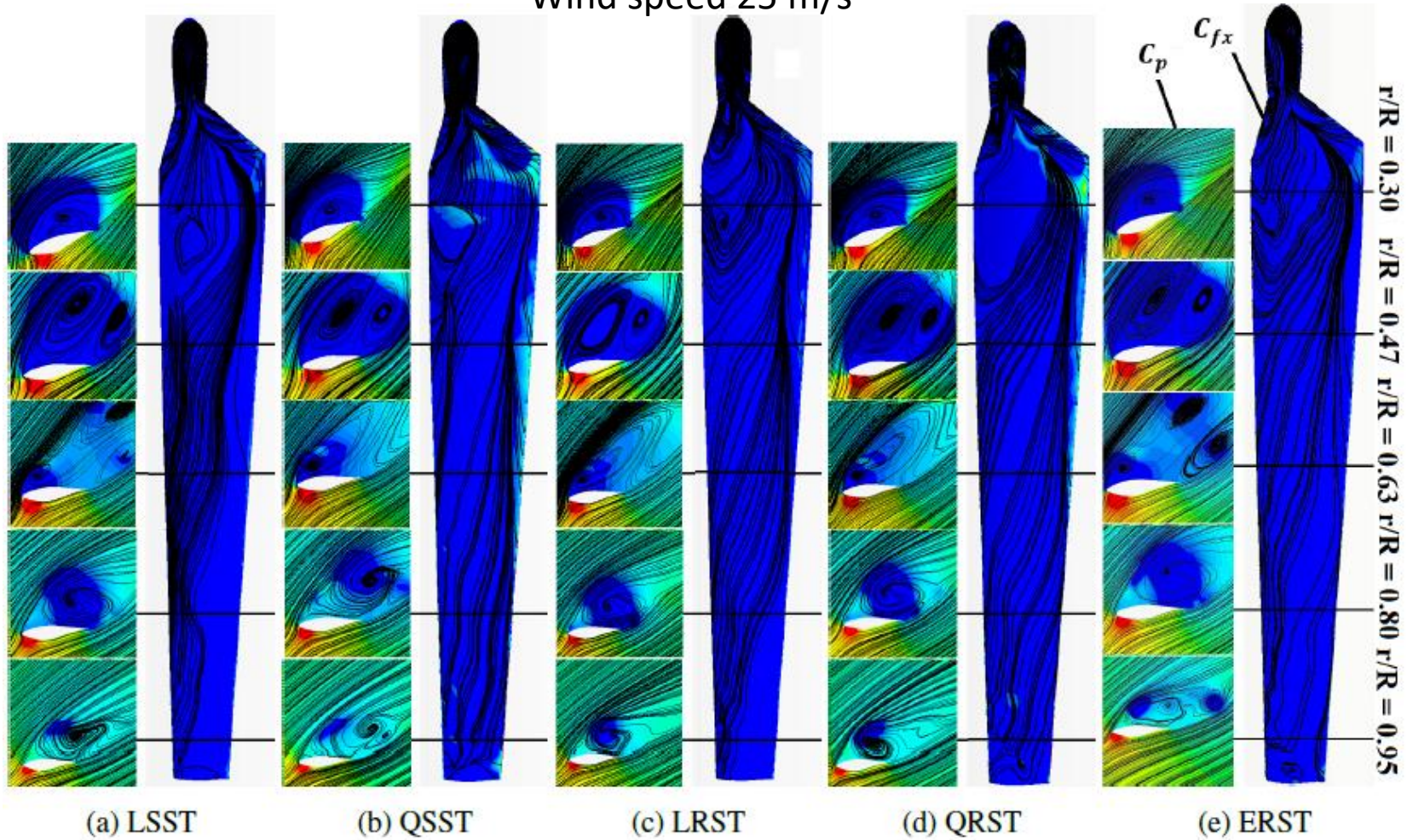
## Flow visualization

Wind speed 15 m/s



## Flow visualization

Wind speed 25 m/s





# Evaluation of the turbulent flow anisotropy

Boussinesq hypothesis

$$\gamma_{\tau} = \text{atan} \left\{ \frac{\tau_{23}}{\tau_{12}} \right\}, \quad \gamma_g = \text{atan} \left\{ \frac{\frac{\partial U_2}{\partial x_3} + \frac{\partial U_3}{\partial x_2}}{\frac{\partial U_1}{\partial x_2} + \frac{\partial U_2}{\partial x_1}} \right\},$$

# Evaluation of the turbulent flow anisotropy

Boussinesq hypothesis

$$\gamma_{\tau} = \text{atan} \left\{ \frac{\tau_{23}}{\tau_{12}} \right\}, \quad \gamma_g = \text{atan} \left\{ \frac{\frac{\partial U_2}{\partial x_3} + \frac{\partial U_3}{\partial x_2}}{\frac{\partial U_1}{\partial x_2} + \frac{\partial U_2}{\partial x_1}} \right\},$$

$$|\gamma_g - \gamma_{\tau}|$$

# Evaluation of the turbulent flow anisotropy

Boussinesq hypothesis

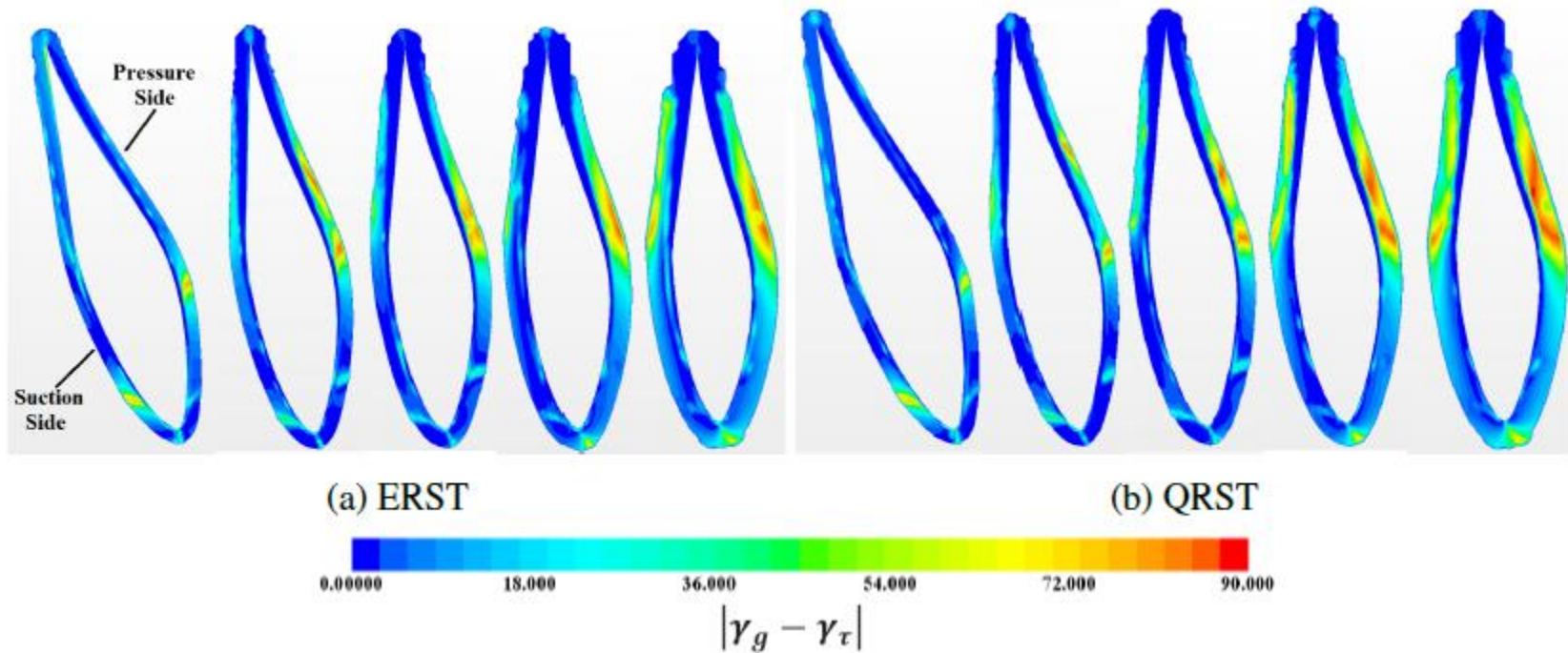
$$\gamma_{\tau} = \text{atan} \left\{ \frac{\tau_{23}}{\tau_{12}} \right\}, \quad \gamma_g = \text{atan} \left\{ \frac{\frac{\partial U_2}{\partial x_3} + \frac{\partial U_3}{\partial x_2}}{\frac{\partial U_1}{\partial x_2} + \frac{\partial U_2}{\partial x_1}} \right\},$$

$$|\gamma_g - \gamma_{\tau}|$$

This evaluation is restricted to the boundary layer region

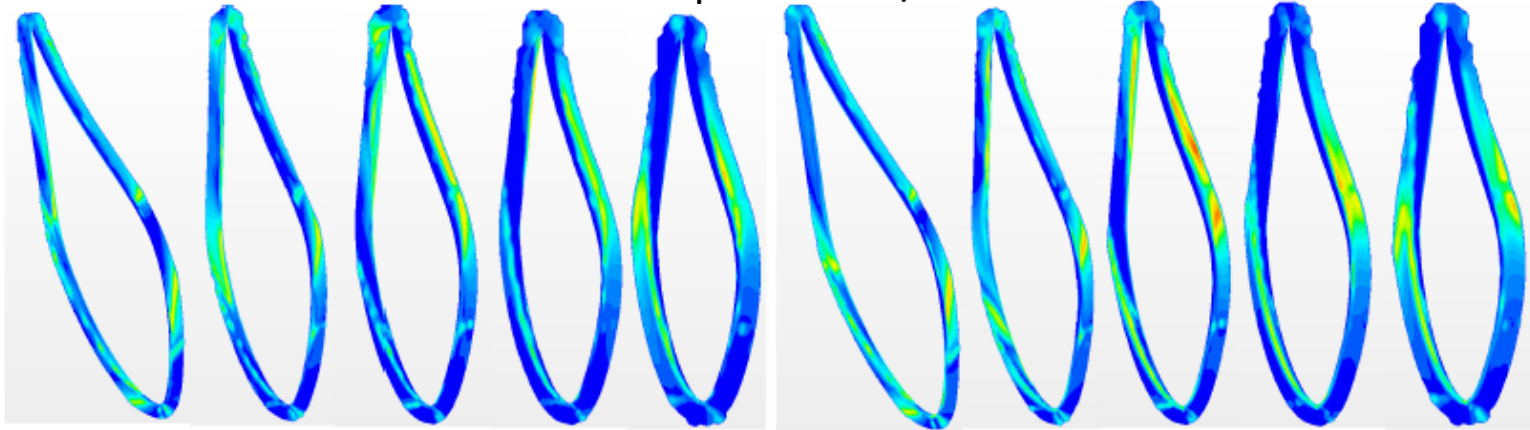
# Evaluation of the turbulent flow anisotropy

Wind speed 5 m/s



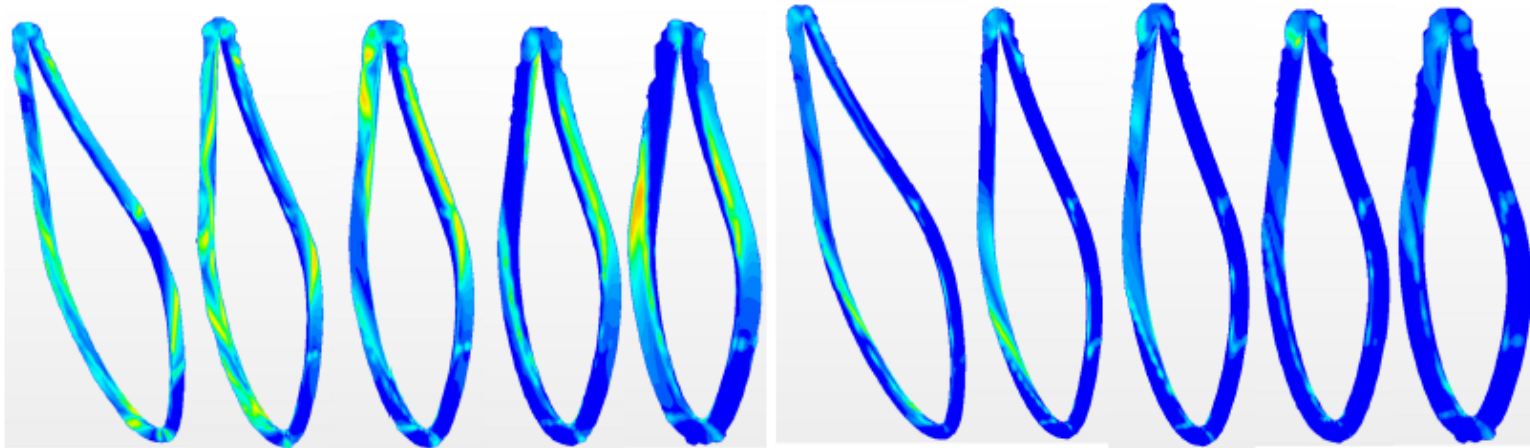
# Evaluation of the turbulent flow anisotropy

Wind speed 10 m/s



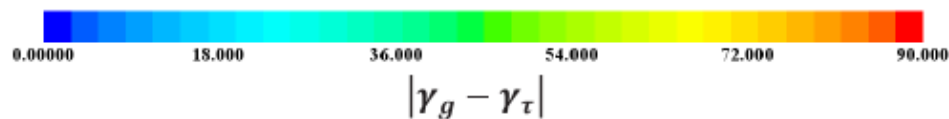
(a) ERST

(b) LRST



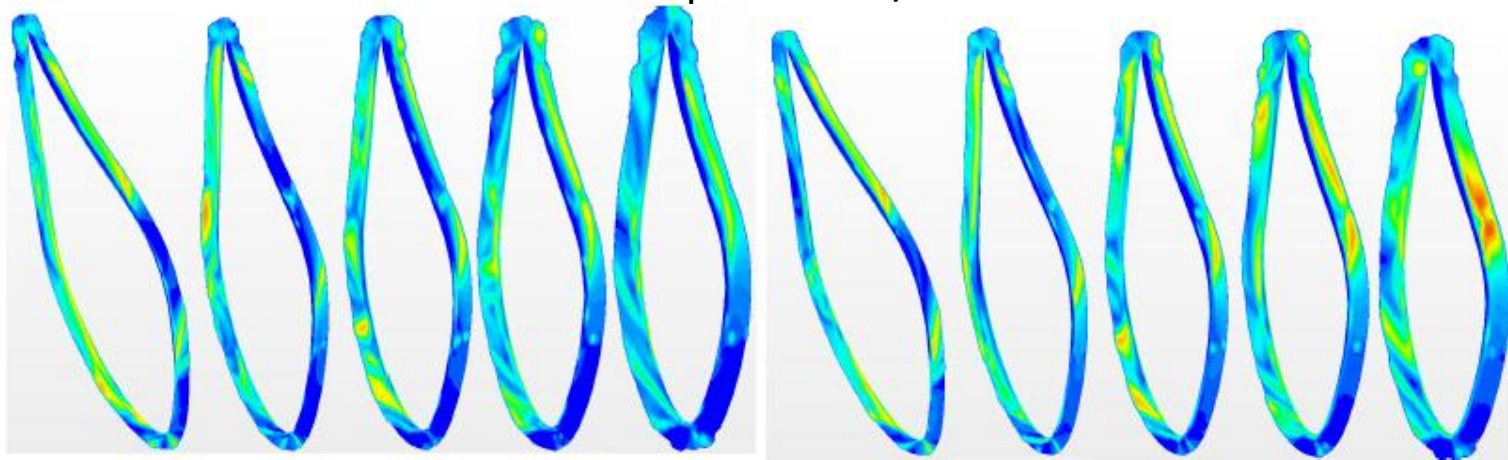
(c) QRST

(d) QSST



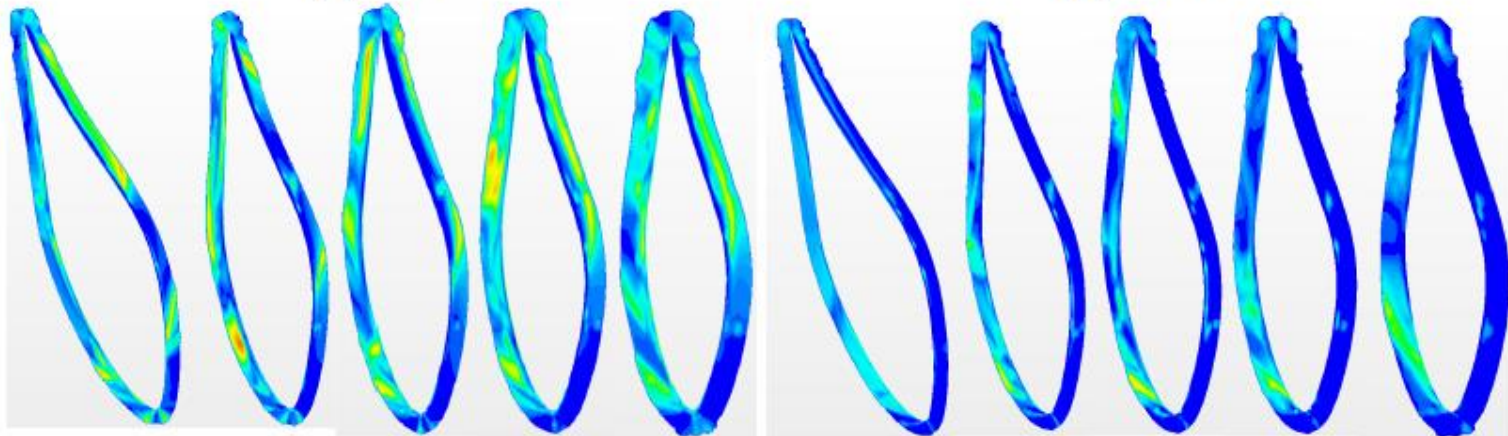
# Evaluation of the turbulent flow anisotropy

Wind speed 15 m/s



(a) ERST

(b) LRST



(c) QRST

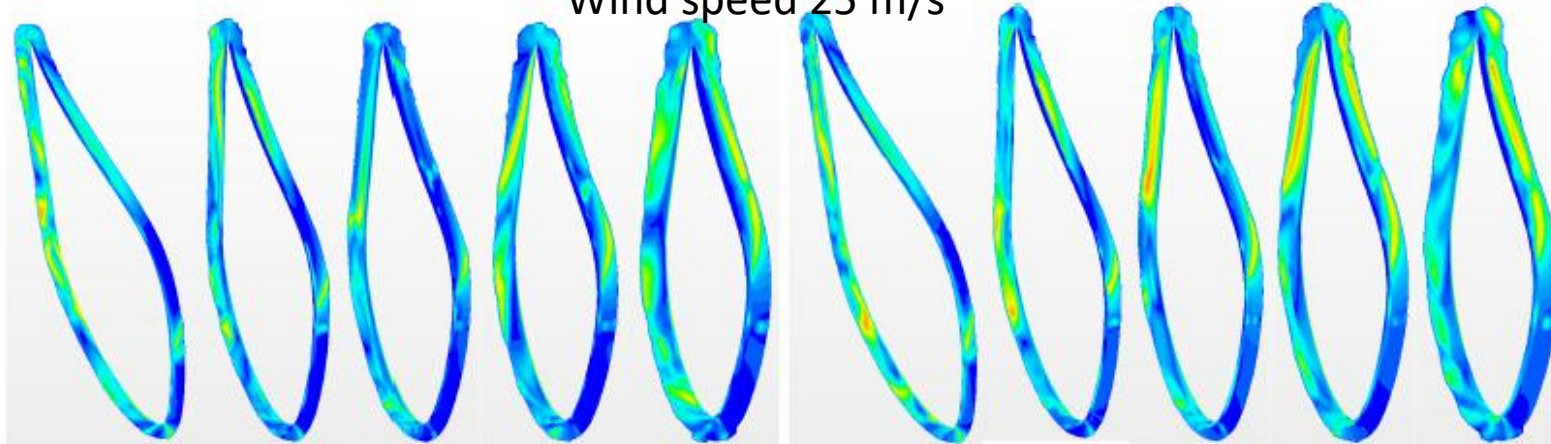
(d) QSST



$$|\gamma_g - \gamma_\tau|$$

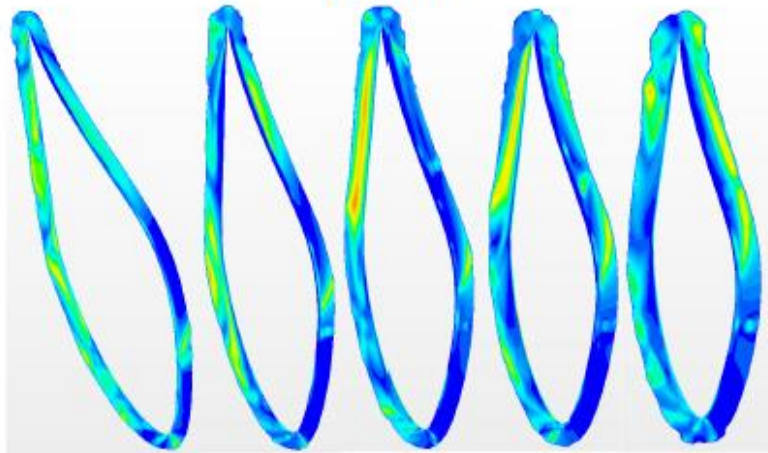
# Evaluation of the turbulent flow anisotropy

Wind speed 25 m/s



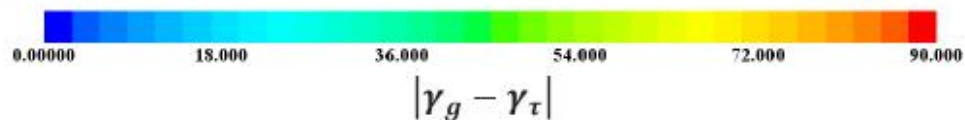
(a) ERST

(b) LRST



(c) QRST

(d) QSST



# Time-dependent variables



# Time-dependent variables

The pressure at blade trailing edge at  $r/R = 0.80$



# Time-dependent variables

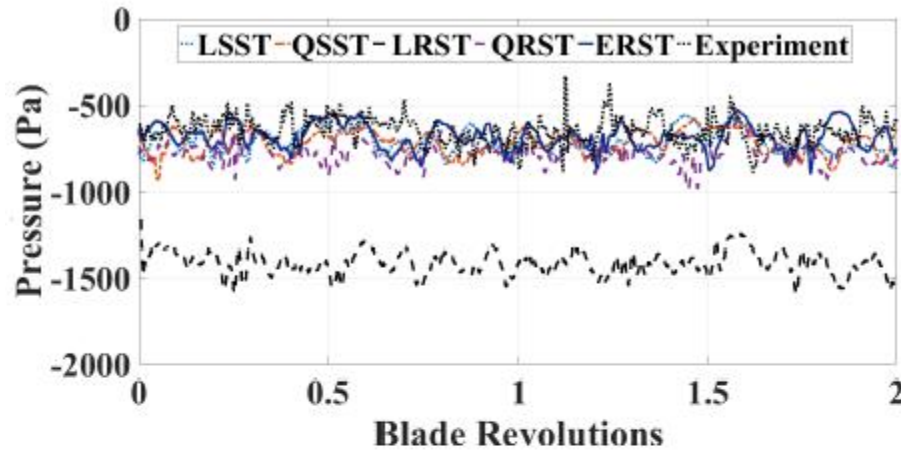
The pressure at blade trailing edge at  $r/R = 0.80$

The thrust

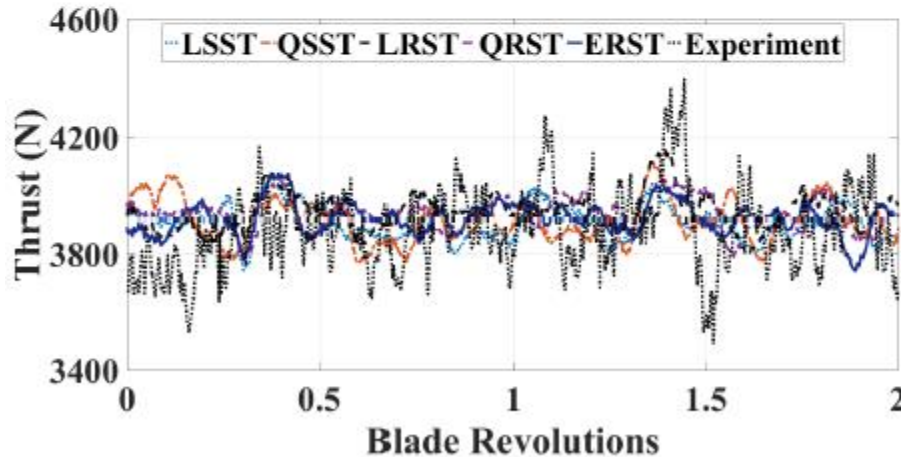
Wind speed 25 m/s



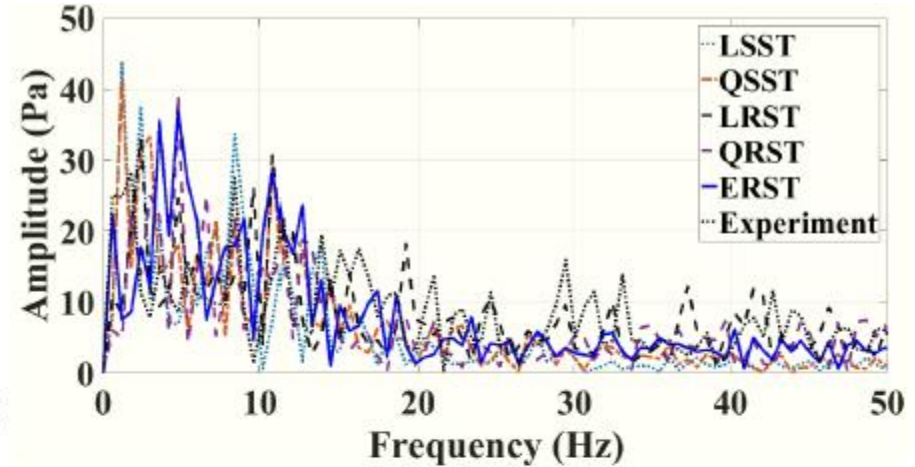
# Time-dependent variables



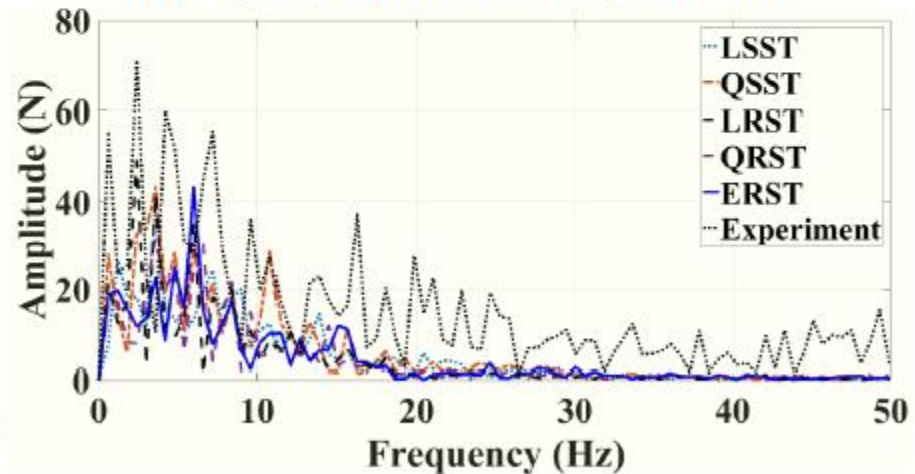
(e) Pressure evolution, wind speed 25 m/s



(g) Thrust evolution, wind speed 25 m/s



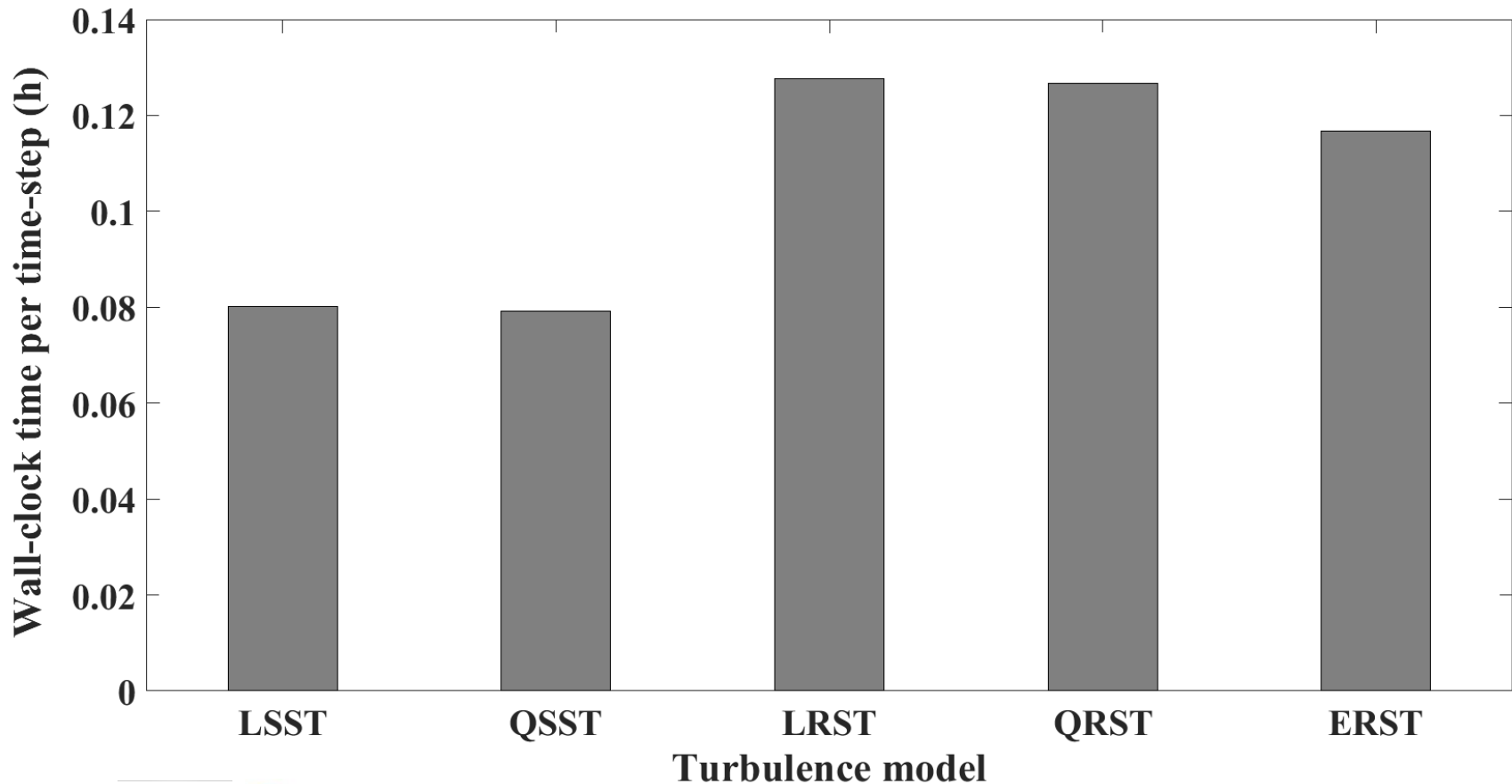
(f) Frequency spectrum, wind speed 25 m/s



(h) Frequency spectrum, wind speed 25 m/s

# Computational cost analysis

The computations are performed on a desktop computer consisting of 64-bit Intel Processors i9-9900KF@ 3.60GHz and 64 GB RAM.





- The RST models, particularly the ERST and QRST, provide consistently more satisfactory predictions.

- The RST models, particularly the ERST and QRST, provide consistently more satisfactory predictions.
- For the wind speed 10 m/s, the turbulence models return different predictions for the extent of the separated flow region over the suction side.

- An evaluation of the Boussinesq hypothesis implies that the turbulence models employing this assumption are inadequate for the prediction of wind turbines aerodynamics.



- An evaluation of the Boussinesq hypothesis implies that the turbulence models employing this assumption are inadequate for the prediction of wind turbines aerodynamics.
- All the models resolve satisfactorily the fluctuation spectrum of the pressure at a single point.

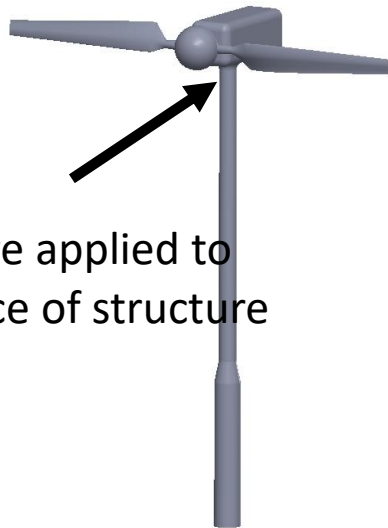
- An evaluation of the Boussinesq hypothesis implies that the turbulence models employing this assumption are inadequate for the prediction of wind turbines aerodynamics.
- All the models resolve satisfactorily the fluctuation spectrum of the pressure at a single point.
- Regarding the thrust force, all the models underestimate the low-frequency fluctuations and also fail to predict the high-frequency fluctuations.

- An evaluation of the Boussinesq hypothesis implies that the turbulence models employing this assumption are inadequate for the prediction of wind turbines aerodynamics.
- All the models resolve satisfactorily the fluctuation spectrum of the pressure at a single point.
- Regarding the thrust force, all the models underestimate the low-frequency fluctuations and also fail to predict the high-frequency fluctuations.
- Finally, the ERST model appears to provide the best trade-off between the accuracy and the computational cost.

# Future Work

## □ Fluid-structure interaction analysis

**Abaqus**



Loads are applied to the surface of structure

Data is exchanged at frequent intervals

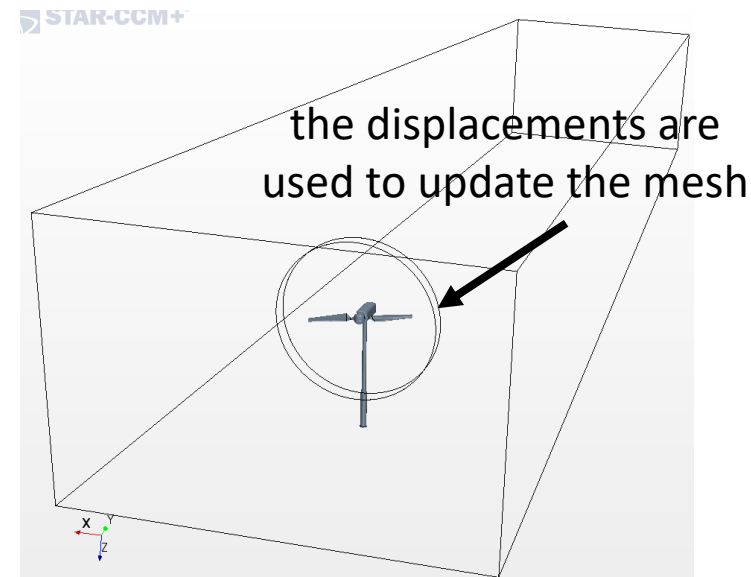
pressure + wall shear stress



displacements



**CFD**



the displacements are used to update the mesh

# Future Work

## Simulações Aerodinâmicas

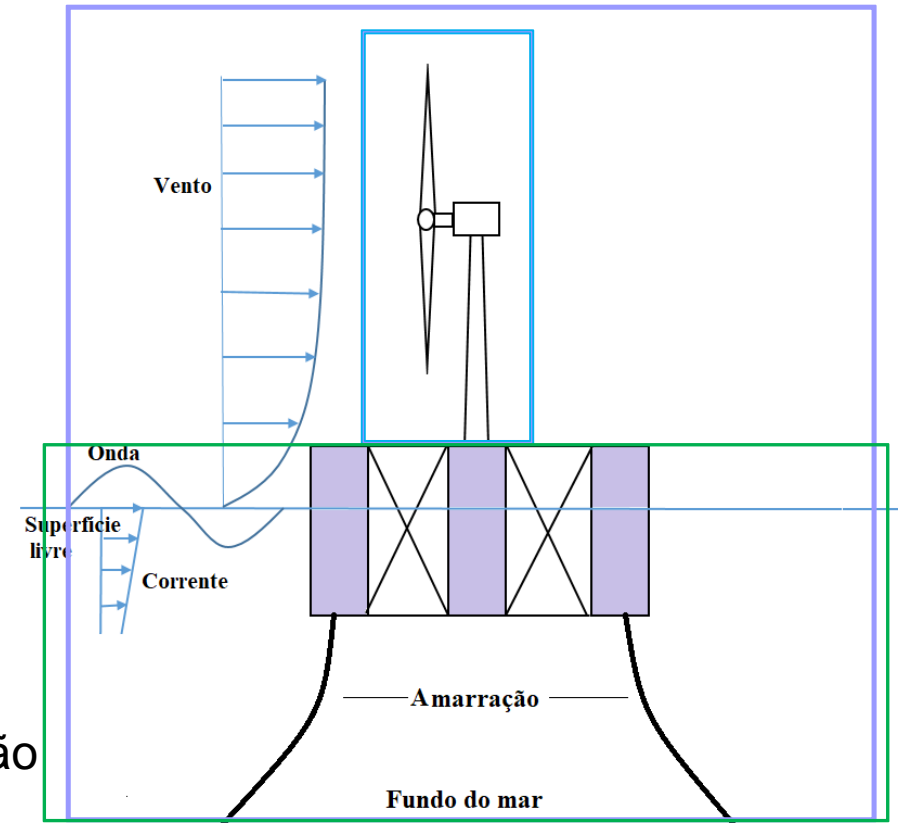
Turbina eólica

## Simulações Hidrodinâmicas

semi-submersível + amarração

## Simulações Hidro-aerodinâmicas

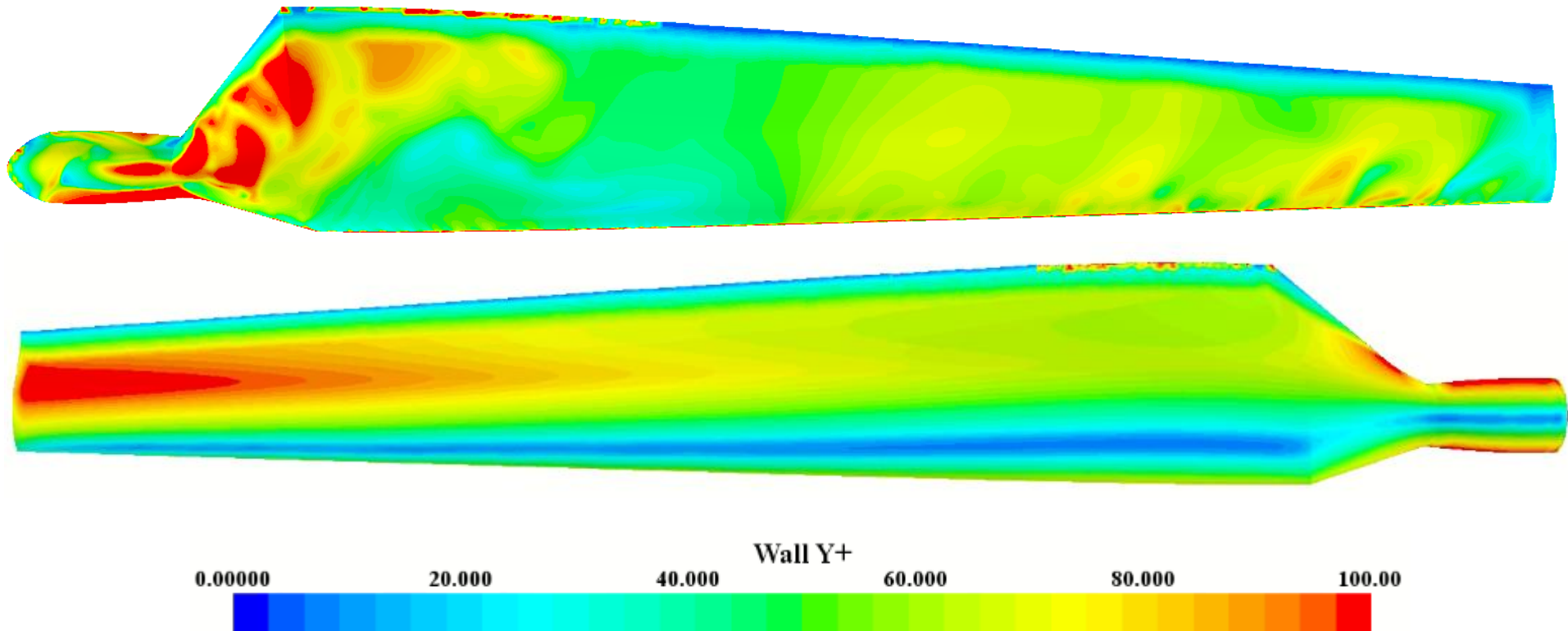
Turbina eólica + semi-submersível + amarração



Numero mínimo de células +  
tamanho do passo de tempo +  
um modelo de turbulência adequado (Modelos não lineares ou  
modelos de Reynolds)

# Future Work

- ❑ Evaluation of the performance of the ERST and LRST models without using the wall function.



# Contributions

## ❑ Submitted Publications

- Amiri M.M., Shadman M., Segen F. Estefen, URANS simulations of a horizontal axis wind turbine under stall condition using Reynolds stress turbulence models, Energy, 2020.



**Questions?**